

Document downloaded from:

<http://hdl.handle.net/10251/202205>

This paper must be cited as:

Costantino, A.; Comba, L.; Cornale, P.; Fabrizio, E. (2022). Energy impact of climate control in pig farming: Dynamic simulation and experimental validation. *Applied Energy*. 309:1-19.  
<https://doi.org/10.1016/j.apenergy.2021.118457>



The final publication is available at

<https://doi.org/10.1016/j.apenergy.2021.118457>

Copyright Elsevier

Additional Information

# Energy impact of climate control in pig farming: dynamic simulation and experimental validation

Andrea Costantino<sup>1,2</sup>, Lorenzo Comba<sup>3,4</sup>, Paolo Cornale<sup>3</sup>, Enrico Fabrizio<sup>1\*</sup>

<sup>1</sup>*DENERG, TEBE Research Group, Politecnico di Torino, Corso Duca degli Abruzzi 24, 10129 Torino, Italy*

<sup>2</sup>*Institute of Animal Science and Technology, Universitat Politècnica de València, Camino de Vera s/n, 46022, València, Spain*

<sup>3</sup>*DISAFA, University of Torino, Largo Paolo Braccini 2, 10095 Grugliasco (TO), Italy*

<sup>4</sup>*CNR-IEIIT, Politecnico di Torino, Corso Duca degli Abruzzi 24, 10129 Torino, Italy*

\*Corresponding author. Tel: +39 011 090 4465;

E-mail address: [enrico.fabrizio@polito.it](mailto:enrico.fabrizio@polito.it)

## Abstract

Pig farming is one of the most energy consuming activities of the livestock sector since a considerable amount of energy is needed in mechanically ventilated pig houses to maintain the adequate indoor climate conditions. This energy consumption is remarkably increasing due to the boost of pork demand +45% between 2010 and 2050- enhanced by socio-demographical changes. The improvement of the energy performance, hence, is becoming more and more a primary target in the path toward an energy-smart food production. Energy simulation models are essential to achieve such ambitious target by enhancing the analysis of energy consumption patterns and the evaluation of potential energy-efficient measures. A well-established and shared energy framework for this specific aim is not present in literature, outlining an important gap that hinders the transition toward an energy-smart agriculture. In this work, a new dynamic energy simulation model is *ad-hoc* developed for the estimation of thermal and electrical energy consumption for climate control of mechanically ventilated growing-finishing pig houses. The strength of the presented model is an accurate simulation of the main peculiarities of pig houses, such as the specific climate control equipment and the pig-environment interactions which are performed through *ad-hoc* calculation modules. The reliability of the model was performed through an experimental validation against real monitored data in compliance with international protocols. The developed model could represent a powerful decision support tool for stakeholders, especially in the design stages of pig houses by favouring the adoption of new technologies in this sector. Through this model, in fact, the impact of new energy-efficient solutions on the energy performance of pig houses can be evaluated in standardized conditions, considering the specific features, such as configuration, geographical location, and farming features.

**Keywords:** dynamic energy simulation model; energy analysis; energy efficiency; livestock buildings; energy smart agriculture; growing-finishing pig houses.

## Nomenclature

$a_{\text{pig}}$	Pig age [days]
$a_{\text{pig\_max}}$	Age of maximum pig growth [days]
$C_m$	Pig house total heat capacity [ $\text{kJ K}^{-1}$ ]
$c_{\text{air}}$	Specific heat capacity of ventilation air [ $\text{J kg}^{-1} \text{K}^{-1}$ ]
$Cv(RMSE)$	Coefficient of Variation of the Root Mean Square Error [%]
$E_{\text{el}}$	Electrical energy consumption [ $\text{kWh}_{\text{el}}$ ]
$E_{\text{th}}$	Therma energy consumption [ $\text{kWh}_{\text{th}}$ ]
$H_{\text{tr\_em}}$	Heat transfer coefficient between external environment and building thermal mass [ $\text{W K}^{-1}$ ]
$H_{\text{tr\_is}}$	Heat transfer coefficient between glazed surface and indoor air [ $\text{W K}^{-1}$ ]
$H_{\text{tr\_ms}}$	Heat transfer coefficient between building thermal mass and building surface [ $\text{W K}^{-1}$ ]
$H_{\text{tr\_fen}}$	Heat transfer coefficient through glazed surfaces [ $\text{W K}^{-1}$ ]
$H_{\text{ve}}$	Ventilation heat transfer coefficient [ $\text{W K}^{-1}$ ]
$h_v$	Enthalpy of water vapour [ $\text{kJ kg}^{-1}$ ]
$IAQ$	Indoor Air Quality
$K_y$	Coefficient of efficiency at weight gain [–]
$k_{\text{bs}_0} - k_{\text{bs}_6}$	Regression coefficients for base ventilation air flow rate calculation
$k_{\text{fan}_0} - k_{\text{fan}_2}$	Regression coefficients for fan airflow calculation
$k_{\text{set}_0} - k_{\text{set}_3}$	Regression coefficients for set point temperature calculation
$k_{\text{SFP}_0} - k_{\text{SFP}_2}$	Regression coefficients for <i>SFP</i> calculation
$\dot{m}_i$	Vapour production from internal sources [ $\text{g}_{\text{vap}} \text{h}^{-1}$ ]
$n_{\text{feed}}$	Feed-related factor [–]
$n_k$	Number of simulation time steps [–]
$n_{\text{pig}}$	Number of pigs inside the house [pigs]
$MBE$	Mean Bias Error [%]
$RH_i$	Indoor air relative humidity [%]
$RH_o$	Outdoor air relative humidity [%]
$RMSE$	Root Mean Square Error
$SFP$	Specific Fan Performance [ $\text{m}^3 \text{Wh}^{-1}$ ]
$U - \text{value}$	Stationary thermal transmittance [ $\text{W m}^{-2} \text{K}^{-1}$ ]
$\dot{V}_{\text{act}}$	Actual ventilation air flow rate [ $\text{m}^3 \text{h}^{-1}$ ]
$\dot{V}_{\text{bs}}$	Base air ventilation flow rate [ $\text{m}^3 \text{h}^{-1}$ ]
$\dot{V}_{\text{cool}}$	Cooling ventilation air flow rate [ $\text{m}^3 \text{h}^{-1}$ ]
$\dot{V}_{\text{fan}}$	Fan airflow rate [ $\text{m}^3 \text{h}^{-1}$ ]
$\dot{V}_{\text{max}}$	Maximum ventilation air flow rate installed in the pig house [ $\text{m}^3 \text{h}^{-1}$ ]
$\dot{V}_{\text{min}}$	Minimum ventilation air flow rate [ $\text{m}^3 \text{h}^{-1}$ ]
$W_{\text{pig}}$	Live weight (body mass) of mature pig [kg]
$w_{\text{pig}}$	Pig live weight (body mass) [kg]
$x_{\text{air}_i}$	Indoor air humidity ratio [ $\text{g}_{\text{vap}} \text{kg}_{\text{air}}^{-1}$ ]
$x_{\text{air}_o}$	Outdoor air humidity ratio [ $\text{g}_{\text{vap}} \text{kg}_{\text{air}}^{-1}$ ]
$\Delta p_{\text{st}}$	Static pressure difference between inside and outside [Pa]
$\Delta \tau$	Duration of the simulation time step [h]
$\delta_{\text{pig}}$	Pig growth rate [ $\text{days}^{-1}$ ]
$\eta_{\text{H}}$	Conversion efficiency of the heating system [–]
$\vec{\theta}$	Vector of temperature
$\theta_{\text{air}_i}$	Indoor air temperature [ $^{\circ}\text{C}$ ]
$\theta_m$	Building mass temperature [ $^{\circ}\text{C}$ ]

$\theta_s$	Temperature of the indoor building surface [ $^{\circ}\text{C}$ ]
$\theta_{\text{set}_C}$	Cooling set point temperature [ $^{\circ}\text{C}$ ]
$\theta_{\text{set}_H}$	Heating set point temperature [ $^{\circ}\text{C}$ ]
$\theta_{\text{set}_{id}}$	Ideal set point temperature [ $^{\circ}\text{C}$ ]
$\theta_{\text{air}_o}$	Outdoor air temperature [ $^{\circ}\text{C}$ ]
$\kappa_i$	Internal aerial heat capacity [ $\text{kJ m}^{-2} \text{K}^{-1}$ ]
$\rho_{\text{air}}$	Volumetric mass density of the ventilation air [ $\text{kg m}^{-3}$ ]
$\tau_k$	k-th simulation time step
$\Phi_{d\_pig}$	Daily feed energy intake of a pig [W]
$\Phi_{C\_nd}$	Supplemental heat load for cooling [W]
$\Phi_{H\_nd}$	Supplemental heat load for heating [W]
$\Phi_{H/C\_nd}$	Supplemental heat load for heating or cooling [W]
$\Phi_{ia}$	Convective heat flow [W]
$\Phi_{lat\_i}$	Latent heat production from internal sources [W]
$\Phi_m$	Radiative heat flow [W]
$\Phi_{m\_pig}$	Heat dissipated by a pig due to maintenance [W]
$\Phi_{sen\_i}$	Sensible heat production from internal sources [W]
$\Phi_{st}$	Radiative heat flow [W]
$\Phi_{tot\_i}$	Total (sensible plus latent) heat production from internal sources [W]

# 1 Introduction

## *1.1 The need of a reduction of the energy consumption in pig farming*

Pork is the greatest meat production at a global level, representing over 40% of the total meat produced worldwide [1]. Around 55% of pork is produced in industrialized production facilities [2] that often are equipped with mechanical climate control systems needed to guarantee the adequate indoor climate conditions to farmed pigs, with positive effects on both production quantity [3] and quality [4]. The use of mechanical systems -e.g. air heaters and fans- entails a considerable energy consumption that contributes to make pig farming the second most energy consuming activity of the entire livestock sector -after milk production- in European Union [5]. In Germany, the EU leader in pork production, the yearly direct energy consumption attributable to pig farming is around 9 PJ, while in Poland -a EU top producer of pork- this energy consumption exceeds 5 PJ per year [5]. Unfortunately, the energy consumption of pig farming is estimated to further increase in the coming future boosted by various sociodemographic changes, such as world population growth and urbanization, that will increase the global demand for pork [6]. According to FAO [7], in fact, pork consumption will increase by 45% before 2050, if compared to the production levels of 2010 [7]. In this context, it is evident that the challenge for the future is not only to produce enough food for meeting the world population demand [8], but the development of innovative food producing systems for a sustainable agriculture is strongly needed [2]. To move toward a more sustainable agriculture, the main sources of energy losses must be assessed [9] and the energy-efficient climate control of pig houses is fundamental due to the high energy consumption that characterize this livestock production and due to the high volume of pork production worldwide.

Consequently, an increasing number of works present in literature is focused on the improvement of the energy performance of pig houses adopting different solutions and technologies. Jackson et al. [10], for example, evaluated the potentialities of incorporating passive technologies in pig house design to decrease the energy consumption. Jeong et al. [11] evaluated the effects of an aerothermal heat pump on the energy efficiency, indoor environment and productivity of a pig house. Alberti et al. [12], analysed the potentialities of the installation of a geothermal heat pump in a piglet nursery, substituting a pre-existing gas air heater. The potentialities of energy saving enhanced by a geothermal heat pump in pig houses were also explored by Islam et al. [13] which evaluated also the potential CO<sub>2</sub> reduction. Krommweh et al. [14] investigated the heating and cooling potential of a modular system for fattening pigs

which integrated a geothermal heat exchanger. Axaopoulos & Panagakis [15] analysed the opportunity to cover the thermal energy demand for supplemental heating in a piglet nursery by using the CH<sub>4</sub> produced through an innovative solar-assisted anaerobic digester. Pipatmanomai et al. [16] analysed the opportunity to adopt a biogas-to-electricity generation systems in a pig farm in Thailand. Axaopoulos et al. [17] analysed the effects of thermal insulation on the heating and cooling transmission heat loads in growing-finishing pig houses.

### *1.2 Energy modelling of pig houses: an important gap*

The efforts towards the improvement of the energy performance for climate control of pig houses could be seriously hindered by the lack of a well-established and shared simulation model specifically developed for the assessment of the energy consumption of this building type. This lack outlines an important gap in literature that should be filled in the perspective of a transition towards an energy-smart food production. In literature, in fact, few models for the simulation of pig houses are present [18], as deeply described in the modelling background of Section 3. Most of the existing models, in fact, were implemented prioritizing or agricultural engineering aspects or energy engineering ones, without filling the gap between these crosscutting research areas. Most of the existing models from agricultural engineering area, in fact, accurately estimate the indoor climate conditions using Computational Fluid Dynamics (*CFD*) [19] without a specific focus on energy consumption. Other models rely on steady-state energy balances that are suitable to size climate control systems in design conditions [20], but not for performing long-term energy analyses. Other models -mainly from energy engineering area- are implemented by apply ready-to-use Building Energy Simulation tools (*BES*) [21], such as TRNSYS and EnergyPlus. The adoption of these ready-to-use tools prevents the accurate simulations of specific aspects of pig houses, such as the time variable indoor air set point temperatures, the presence of free cooling systems and the high values of internal heat and moisture production from internal sources. For example, a 170 kg pig reared at 20 °C of indoor air temperature can produce up to 150 W of sensible heat and up to 130 g h<sup>-1</sup> of water vapour, according to the formulations provided by Pedersen & Sällvik [23]. The lack of a simulation model specifically developed for estimating the energy consumption of pig houses has a negative impact especially on the energy-efficient design of pig houses. In the current practice, in fact, the design process of pig houses -and, in general, of livestock houses [22]- is a shallow process that provides the same standardised solutions for different contexts, without exploring the opportunities that fine-tuned design solutions could provide in improving the

energy performance. The lack of a similar energy simulation model hinders the wide adoption in pig sector of new energy-efficient technologies developed by manufacturers. Currently, in fact, the effectiveness of these new technologies is evaluated through expensive lab tests or on-field experimentations, with results that are dependent on the testing conditions and are complex to be generalized, making also challenging an accurate estimation of the pay-back period for the farmer's investment. By contrast, a reliable energy simulation model would enhance the assessment of the effectiveness of these solutions in standardized conditions through *ad-hoc* simulations that can be calibrated on the very own features of the considered pig house.

### *1.3 Aim, novelty, and structure of the work*

The objective of this work is to propose a novel energy simulation model specifically developed and validated for estimating the energy consumption of mechanically ventilated growing-finishing pig houses. The presented work contributes to the new body of knowledge by providing a new customized energy simulation model that does not rely on a ready-to-use Building Energy Simulation tool and that includes the simulation of specific aspects of pig houses, such as pig-environment interactions and specific climate control systems, through *ad-hoc* developed calculation modules. Only considering these peculiarities, in fact, mechanically ventilated growing-finishing pig houses -complex thermodynamic systems that deeply differ from other building types- could be properly simulated. Mechanically ventilated growing-finishing pig houses were selected among other types of pig buildings –e.g. farrowing houses and pig nursery houses– because they are very widespread and the presence of mechanical systems entail higher energy consumption than naturally ventilated houses.

The work is structured as it follows. All the peculiarities of growing finishing pig houses that make them worth of interest from the modelling point of view are clarified in section 2. In section 3, a literature background focused on the existing simulation models for pig houses is provided and the differences with the presented model are highlighted. In sections 4 and 5, the model development and validation are presented, respectively, while in section 6 an example of application is shown to illustrate the potentialities of the proposed model. The final remarks of this work are presented in section 7.

## **2 Peculiarities in the simulation of growing-finishing pig houses**

In this section, the main peculiarities that have to be considered in the energy simulation of growing-finishing pig houses are presented. These peculiarities regard both the building and the climate control systems typical of growing-finishing pig houses.



## *2.1 Peculiarities of buildings for growing-finishing pigs*

In the last stage of their production cycle, pigs are reared in growing-finishing houses to reach the target final live weight, that can be around 100 kg for butcher's meat production or around 160 kg for cured meat production, depending on the country and market needs [24]. Usually, intensive growing-finishing pig houses are totally confined livestock systems that, inside, are divided in pens in which pig are reared in groups that are kept together since weaning stage, to decrease fights and stress problems [25]. The opaque envelope of growing-finishing pig houses is made of masonry -especially in outdated houses- or prefabricated panels -recently built houses- that are more and more preferred due to the easy installation, high durability, good thermal properties, and low cost. Windows are made up of polycarbonate hollow sheet panels and their opening can be managed by automatized electric systems to maintain a constant value of static pressure difference ( $\Delta p_{st}$ ) between inside and outside the house.

Partially or completely slatted floor systems are widespread in growing-finishing pig houses because they allow manure to be easily collected into pits under the floor, reducing the labour requirements [26]. Once in the pits, manure can be removed at the end of the production cycle or it can be frequently flushed, minimizing the bacterial digestion and the consequent gas production with positive effects for the Indoor Air Quality (*IAQ*) of the house [25].

## *2.2 Peculiarities of climate control in growing-finishing pig houses*

In mechanically ventilated growing-finishing pig houses, climate control systems maintain the adequate indoor climate conditions needed to guarantee animal welfare and to improve the production. From an operative point of view, a range of indoor air temperatures ( $\theta_{air,i}$ ) between 21 and 16 °C is considered the optimal one to improve pig welfare and to increase their productivity [27]. Nevertheless, it could be difficult to guarantee these indoor air temperatures especially during the warm season since only free cooling systems are present in pig houses, as shown later in this section. The optimal range of relative humidity ( $RH_i$ ) is between 60% and 75% [27,28]. Lower values of  $RH_i$  should be avoided since they could cause airway dryness and dehydration in pigs, facilitating the occurrence of respiratory problems. Higher  $RH_i$  values combined with low  $\theta_{air,i}$  can rise the skin thermal conductivity, increasing the occurrence of cold stress situations during the cool season. During the warmer season, higher  $RH_i$  values with high  $\theta_{air,i}$  can hindered the heat dissipation of pigs, increasing the occurrence of heat stress situations [29]. Heat stress is a detrimental condition for pigs from the ethic point of view since animal welfare can be considerably affected. Heat stress is also negative from the financial

point of view, since it decreases productive performance -i.e., worse feed conversion ratio- and may lead to an increase mortality [30]. This is since pigs suffering from heat stress adopt phenotypic responses, such as a reduction of feed intake. In addition, most of the energy obtained by the intake feed is used to maintain homeothermy and not for growth, with a consequent decrease in weight gain [31]. St-Pierre et al. [32] estimated that, in USA, heat stress causes around 0.6% of the death among growing-finishing pigs and a reduction in weight gain up to 7 kg head<sup>-1</sup> each year. The economic loss due to the consequences of heat stress can be estimated around \$202 million yearly [32].

To maintain the previously presented adequate indoor climate conditions, mechanical systems are usually adopted in growing-finishing pig houses. Supplemental heating is provided by air heaters or hot water systems. In many growing-finishing pig houses, mechanical ventilation is adopted to cool the farmed pigs. During the warmest periods, high ventilation air flow rates are provided to remove the heat produced by pigs and to decrease  $\theta_{\text{air}_i}$  by inletting cooler outdoor air. Mechanical ventilation is also a good strategy to control *IAQ* by diluting and removing the contaminants through fresh outdoor air. The high indoor concentration of aerial dust particles, gases and odorous vapours, in fact, can affect pig health and can create a potentially hazardous environment for workers [33]. In growing-finishing pig houses equipped with slatted floor, exhaust ventilation systems are the most widespread ones [34], especially the so-called “pit ventilation” strategy. In pit ventilation, indoor air is exhausted by fans placed below the slatted floor level, enhancing the fresh air to inlet from openings placed in the rearing area [34]. Being exhausted below the floor level, the contact between noxious gases, originated in the pits, and the pigs’ snouts, that are close to the floor, is avoided [33]. Since mechanical ventilation is performed, air velocity inside the pig house should be carefully controlled to avoid drafts. Pigs, in fact, are strongly affected by temperature variations and draft due to the lack of a protective layer on their skin due to the absence of hair [25]. Usually, the air velocity around pigs should be between 0.2 and 1.5 m s<sup>-1</sup> as a maximum value to avoid welfare problems. Higher air speeds are well tolerated in presence of high  $\theta_{\text{air}_i}$  -summer conditions- because they enhance the heat dissipation from the pig body [34].

### **3 Modelling background for pig house simulations**

In literature, different types of pig house models were developed with different purposes, as visible from Table 1 where the main pig house models present in literature are reported. As visible from the table, several models adopt Computational Fluid Dynamics (*CFD*) to deeply analyse the entire spatial domain of the enclosure from the point of view of indoor climate

conditions, but without a specific focus on energy consumption. Seo et al. [35] developed a *CFD* model to investigate the ventilation problems of a pig house during the cold season, with a special focus on the simulation of pigs and on the configurations of the ventilation system to improve the reliability of the model. Kwon et al. [36] developed a *CFD* model to evaluate the efficiency of pipe-exhaust systems in reducing dust emission during feed supply in pig nursery houses. Bjerg et al. [37] used *CFD* simulations to predict the indoor effective temperature in the lying area of a growing-finishing pig houses equipped with hinged ceiling flap inlet, exploring the potentialities of this inlet type for controlling the indoor air velocity. Rong & Aarnink [38] used *CFD* simulations to derive the  $\text{NH}_3$  mass transfer coefficients above metal and concrete slatted floor in an experimental pig house. Rong [39] applied a validated *CFD* model for investigating the removal ratio of  $\text{NH}_3$  emissions in a pig house with pit ventilation. Tabase et al. [19] developed a *CFD* model to predict the indoor air flow and  $\text{NH}_3$  distribution in a pig house equipped with an underfloor air distribution system. The *CFD* model of Qin et al. [40] investigated the effects of slatted floor layouts on the airflow pattern in a manure pit and the consequent  $\text{NH}_3$  emissions. As just shown, *CFD* are widely used to analyse in detail the indoor environmental conditions of pig houses, focusing on aspects such as ventilation and  $\text{NH}_3$  emissions. By contrast, *CFD* models are not used to assess the energy performance of pig houses. This is mainly due to the high computational time required for long-term simulations and due to the complexity in modelling climate control systems of pig houses.

**Table 1** – Scientific works present in literature focused on pig house modelling.

Reference	Publication year	Model type	Focus
Seo et al. [35]	2012	<i>CFD</i> model	Ventilation
Kwon et al. [36]	2016	<i>CFD</i> model	Dust emission
Bjerg et al. [37]	2018	<i>CFD</i> model	Indoor effective temperature
Rong & Aarnink [38]	2019	<i>CFD</i> model	$\text{NH}_3$
Rong [39]	2020	<i>CFD</i> model	$\text{NH}_3$ removal ratio
Tabase et al. [19]	2020	<i>CFD</i> model	Ventilation and $\text{NH}_3$
Qin et al. [40]	2020	<i>CFD</i> model	Ventilation and $\text{NH}_3$
Albright [20]	1990	Steady-state model	Climate control system sizing
Lindley & Whitaker [25]	1996	Steady-state model	Climate control system sizing
Axaopoulos et al. [17]	2014	<i>BES</i> model	Thermal insulation
Jackson et al. [21]	2017	<i>BES</i> model	Pig house design improvement
Jackson et al. [10]	2018	<i>BES</i> model	Pig house design improvement
Axaopoulos et al. [41]	1992	<i>Ad-hoc</i> model	Heat stress
Liberati & Zappavigna [42]	2005	<i>Ad-hoc</i> model	Indoor climate conditions
Wu et al. [43]	2006	<i>Ad-hoc</i> model	Indoor air temperature and energy consumption

Panagakos & Axaopoulos [44]	2008	<i>Ad-hoc</i> model	Fogging strategies
Xie et al. [45]	2019	<i>Ad-hoc</i> model	Indoor climate conditions and energy consumption

To analyse energy-related aspects, lumped-parameter models are preferred. These models, in fact, can estimate the thermal and electrical energy consumption for climate control and the average lumped indoor climate conditions, mainly  $\theta_{\text{air},i}$  and  $RH_i$ . The simplest lumped-parameter models are the steady-state ones that are usually adopted to perform simplified energy calculations. These models, which formulation is suitable for several types of livestock houses, are present in the main handbooks of agricultural engineering, such as the ones of Albright [20] and Lindley & Whitaker [25]. As reported in Table 1, steady-state energy models are mainly used for sizing the climate control system -e.g. number of fans and heating capacity- and for evaluating the potential animal heat stress risk under given steady-state boundary conditions. The excessive simplifications that characterize the steady-state energy models make them not suitable for the estimation of the energy consumption of pig houses. For this reason, dynamic energy simulation models are preferred [46].

Most of the dynamic energy simulation models used to simulate pig houses are implemented in ready-to-use Building Energy Simulation (*BES*) tools, such as EnergyPlus or TRNSYS. *BES* tools enhance the possibility to solve the energy and moisture balances through pre-set equations that consider in detail complex phenomena, such as the dynamic behaviour of the building and the radiative heat exchange. Since *BES* tools were specifically developed for “civil” buildings, such as housing and offices, the simulation of the thermal environment of pig houses could be complex. This is because tough modifications are required to simulate the specificities of this building type, such as the specific climate control equipment and the pig thermal emission. These tough modifications hindered the use of *BES* tools for pig house simulations. Nevertheless, examples of *BES* tools used to simulate pig houses are present in literature. Axaopoulos et al. [17] developed an energy simulation model in TRNSYS which objective was the evaluation of the optimum insulation thickness of growing-finishing pig house walls, considering different orientations and compositions of these building components. Jackson et al. [21] developed an EnergyPlus model for improving the design of pig housing to promote the efficient use of resources and to enhance animal welfare. The same model was adopted in [10] to improve the pig house design, by including passive design techniques to reduce the time that pigs spend in not adequate indoor climate conditions.

Finally, pig houses can be simulated using *ad-hoc* developed models that rely on a set of customized equations to solve thermal and moisture balances. *Ad-hoc* developed models have

the advantage of considering all the specificities typical of pig houses, they can simulate the climate control systems typical of these buildings and they can be fine-tuned for the specific purposes of the performed analyses. These features make ad-hoc models a very suitable option for the implementation of a dynamic thermal model for the estimation of energy performance of pig houses. Models for pig houses were *ad-hoc* developed for different purposes. Axaopoulos et al. [41] developed a thermal model for simulating the thermal microenvironment of growing pigs under summer conditions with a special focus on the assessment of potential heat stress situations for pigs. Similarly, Liberati & Zappavigna [42] developed and validated a dynamic energy model for optimising the indoor climate conditions in pig houses. Both the previous models ([41,42]) were focused on indoor climate conditions, without assessments of energy consumption. Wu et al. [43] developed a predictive control model for generic livestock houses with the aim of improving the regulation of the indoor air temperature and minimizing the energy consumption. Panagakis & Axaopoulos [44] developed a dynamic energy simulation model to evaluate the effectiveness of different fogging strategies aimed at avoiding pig heat stress. The model estimated heat stress indices and water consumption, but no energy consumption was estimated. Xie et al. [45] developed and compared two models for estimating the indoor climate conditions of a pig house. The first model was a dynamic energy model based on energy balance equations, while the second one was a data-driven model based on a neuro fuzzy inferring system. The results of that work showed that the first model better estimated the indoor air temperature and, therefore, it was used for the estimation of the pig house energy consumption.

This analysis shows that different pig house simulation models are present in literature, but there is an important gap concerning models that are *ad-hoc* developed for the estimation of energy consumption for climate control. In the following sections, a lumped-parameter dynamic model for estimating the indoor climate conditions and energy consumption of growing-finishing pig houses is presented and validated.

## **4 Pig house energy model: development**

### *4.1 General structure of the model*

The presented energy simulation model, implemented in MATLAB<sup>®</sup> environment, can be schematised into five calculation modules (Figure 1), namely

- Initialization module;
- Pig modelling module;
- Thermal balance module;

- Moisture balance module;
- System efficiency module.

To start an energy simulation using the presented model, input data should be provided. They regard mainly the geometrical and thermophysical properties of the pig houses, the farming features and the outdoor weather conditions. The calculation starts with the “Initialization module” that calculates all the variables needed in the following modules -e.g. heat transfer coefficients and the total building fabric heat capacity- starting from the input data. Then, the model starts a calculation loop that is repeated per each  $k$ -th simulation time step. This loop begins with the “Pig modelling module” that estimates the time-dependant variables, such as the pig live weight and the heat and moisture production at house level. The calculated boundary conditions are needed to solve the thermal balance (“Thermal balance module”) to estimate  $\theta_{air,i}$ . The obtained  $\theta_{air,i}$  is compared with the heating ( $\theta_{set,H}$ ) and cooling ( $\theta_{set,C}$ ) set point temperatures and three main cases can occur, as shown by Figure 1:

- $\theta_{set,H} \leq \theta_{air,i} \leq \theta_{set,C}$ : in this first case,  $\theta_{air,i}$  is in free-floating conditions and neither heating nor cooling loads are needed. The model follows the workflow and estimates  $RH_i$  through the “Moisture balance module”;
- $\theta_{air,i} < \theta_{set,H}$ : in this second case, a supplemental heating load is needed and it is estimated by solving the thermal balance. The model updates the thermal balance with the calculated supplemental heating load and then, estimates  $RH_i$  through the “Moisture balance module”;
- $\theta_{air,i} > \theta_{set,C}$ : in this third case, a cooling load is needed and it is estimated by solving the thermal balance. The obtained cooling load is theoretical and it has to be converted in an equivalent ventilation flow rate to maintain  $\theta_{set,C}$  since no mechanical cooling systems are usually present in pig houses. The model updates the thermal balance considering the new ventilation flow rate and then, estimates  $RH_i$  through the “Moisture balance module”.

The last step of the calculation loop is the “System efficiency module” in which the hourly thermal and electrical energy consumptions for climate control are calculated considering the system efficiency. After that, the model starts the simulation of the next time step, beginning again from the “Pig modelling module”.

At the end of the calculation, the model provides the thermal and electrical energy consumption for climate control over the entire simulation period. The hourly values of  $\theta_{air,i}$  and  $RH_i$  are further valuable outputs of the model.

In the following sections, the calculation modules of the presented model are described more in detail.

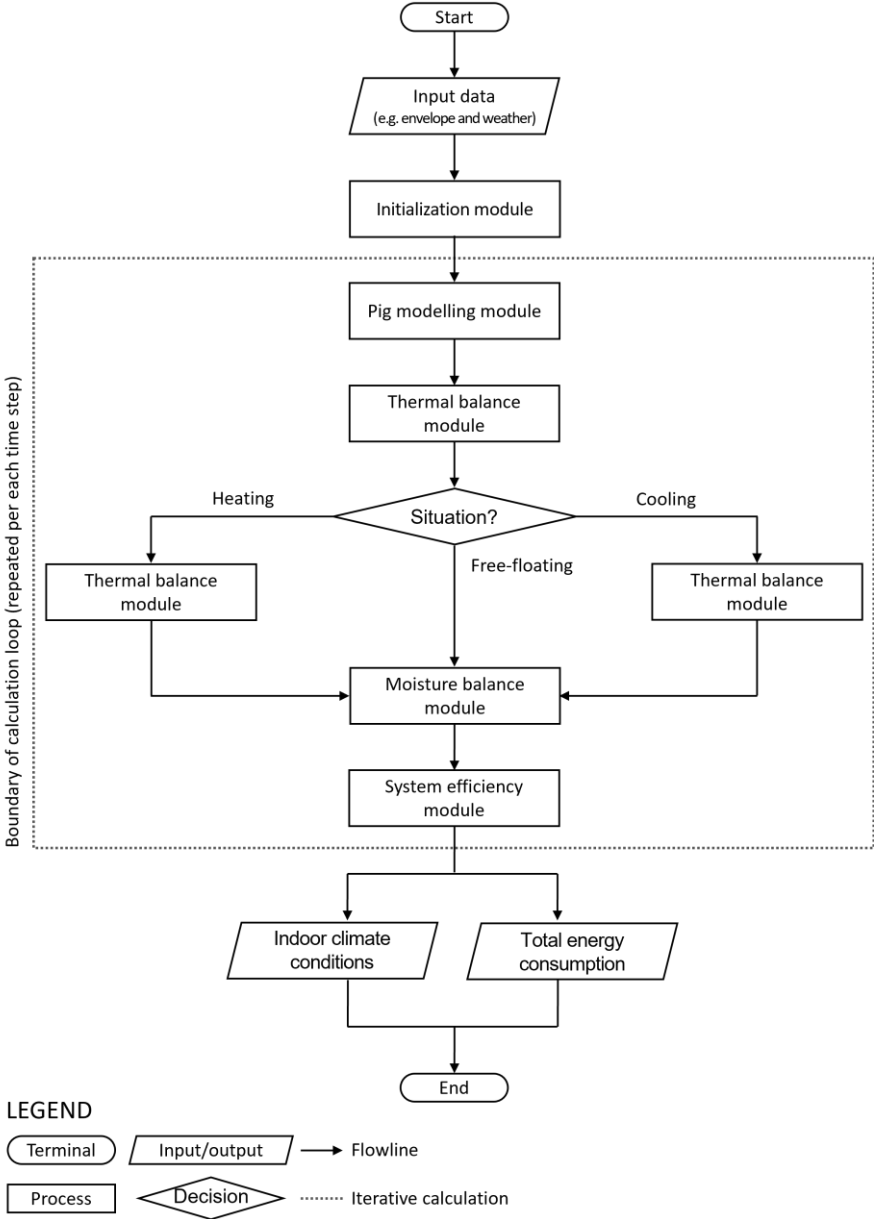


**Figure 1** - Calculation modules and workflow of the developed model. The workflow contained in the dotted contour is repeated for each time-step of the simulation.

4.2 Main processes of the model

4.2.1 Initialization module

The purpose of this module is to calculate all the variables that are needed for the simulation starting from the input data, such as the heat transfer coefficients and the equivalent solar areas.

#### 4.2.2 Pig modelling module

The ‘‘Pig modelling module’’ is needed to estimate the time-dependent boundary conditions specifically related to pigs. Aspects such as pig thermal and vapour emissions, in fact, should be accurately estimated to solve the thermal and moisture balances.

In the developed model, all the needed boundary conditions are expressed as a function of pig body mass ( $w_{\text{pig}}$ ), commonly known as pig live weight. Since the presented model is dynamic,  $w_{\text{pig}}$  is calculated daily as a time-dependant variable for precisely considering the variations of the boundary conditions that are dependent on pig growth. The estimation of  $w_{\text{pig}}$  as a function of pig age ( $a_{\text{pig}}$ ) is a task that was faced by several Authors in literature and different functions were developed and analysed [47]. According the results of two different studies [48,49], the Gompertz function [50] was proved to be a reliable relation for  $w_{\text{pig}}$  estimation. At generic  $k$ -th simulation time step  $\tau_k$ , this function -adapted from [48]- reads

$$w_{\text{pig}} = W_{\text{pig}} \cdot e^{\left(-e^{\left(-\delta_{\text{pig}} \cdot (a_{\text{pig}}(\tau_k) - a_{\text{pig\_max}})\right)}\right)} \quad [\text{kg}] \quad (1)$$

where  $W_{\text{pig}}$  is the live weight (body mass) of mature pig (kg),  $\delta_{\text{pig}}$  is pig growth rate ( $\text{days}^{-1}$ ) and  $a_{\text{pig\_max}}$  is the age of maximum pig growth (days). The term  $a_{\text{pig}}(\tau_k)$  represents pig age (days) calculated at the  $k$ -th time step  $\tau_k$ . The values of the three constant  $W_{\text{pig}}$ ,  $\delta_{\text{pig}}$  and  $a_{\text{pig\_max}}$  are related to the considered pig breed and can be obtained by fitting the function of Eq.(1) on real growing data provided by farmers or obtained from literature.

Heat and moisture production from internal sources can be expressed as a function of  $w_{\text{pig}}$ . In the framework of this work, heat and moisture production are estimated referring to the specific formulations for growing-finishing pig houses provided in [23]. These formulations estimate heat and moisture production at house level. Therefore, they include not only heat and moisture produced directly by pigs but even water evaporation from feed, waterers, and manure. The total -sensible *plus* latent- thermal emission from internal sources ( $\phi_{\text{tot\_i}}$ ) can be expressed at each time step through the following formulation adapted from [23]

$$\phi_{\text{tot\_i}} = \frac{\{[\phi_{\text{m\_pig}} + (1 - K_y) \cdot (\phi_{\text{d\_pig}} - \phi_{\text{m\_pig}})] \cdot (1240 - 12 \cdot \theta_{\text{air\_i}})\} \cdot n_{\text{pig}}}{1000} \quad [\text{W}] \quad (2)$$

where  $\phi_{\text{m\_pig}}$  is the heat dissipated by a single pig due to maintenance (W),  $K_y$  is the dimensionless coefficient of efficiency at weight gain,  $\phi_{\text{d\_pig}}$  is daily feed energy intake by a pig (W),  $\theta_{\text{air\_i}}$  is the indoor air temperature ( $^{\circ}\text{C}$ ) and  $n_{\text{pig}}$  is the number of pigs present inside the house. The term  $\phi_{\text{m\_pig}}$  is a function of  $w_{\text{pig}}$  and reads



$$\Phi_{m\_pig} = 5.09 \cdot w_{pig}^{0.75} \quad [W] \quad (3)$$

The dimensionless coefficient  $K_y$  is also function of  $w_{pig}$  and reads

$$K_y = 0.47 + 0.003 \cdot w_{pig} \quad [-] \quad (4)$$

The daily feed energy intake by a pig can be expressed as

$$\Phi_{d\_pig} = n_{feed} \cdot \Phi_{m\_pig} \quad [W] \quad (5)$$

where  $n_{feed}$  is a dimensionless factor which values for country and rate of gain are reported in [23]. Please note that being  $\Phi_{tot\_i}$  function of  $\theta_{air\_i}$ , the computation of this last parameter by solving the thermal balance is performed iteratively.

According to [23], the sensible heat emission from internal sources ( $\Phi_{sen\_i}$ ) can be calculated as

$$\Phi_{sen\_i} = \{ [0.62 \cdot (1240 - 12 \cdot \theta_{air\_i})] - 1.15 \cdot 10^7 \cdot \theta_{air\_i}^6 \} \cdot n_{pig} \quad [W] \quad (6)$$

Once obtained  $\Phi_{tot\_i}$  and  $\Phi_{sen\_i}$ , the latent heat emission from internal sources ( $\Phi_{lat\_i}$ ) can be calculated as the difference between  $\Phi_{tot\_i}$  and  $\Phi_{sen\_i}$ . Knowing  $\Phi_{lat\_i}$ , the vapour emission from internal sources ( $\dot{m}_i$ ) is obtained as

$$\dot{m}_i = \frac{\Phi_{lat\_i} \cdot 3.6}{h_v} \quad \left[ \frac{kg_{vap}}{h} \right] \quad (7)$$

where  $h_v$  is the enthalpy of water vapour ( $kJ \, kg^{-1}$ ) calculated at  $\theta_{air\_i}$  temperature.

At each simulation time step, the model estimates the ideal set point temperature ( $\theta_{set\_id}$ ) as a function of  $w_{pig}$  through the following piecewise-defined function

$$\theta_{set\_id}(w_{pig}) = \begin{cases} g(w_{pig}) & w_{pig} < 90 \\ 14.4 & w_{pig} \geq 90 \end{cases} \quad (8)$$

with

$$g(w_{pig}) = k_{set\_3} \cdot w_{pig}^3 + k_{set\_2} \cdot w_{pig}^2 + k_{set\_1} \cdot w_{pig} + k_{set\_0} \quad [^\circ C] \quad (9)$$

where  $k_{set\_3} - k_{set\_0}$  are the polynomial regression coefficients obtained from [27] and reported in Table 2. The heating ( $\theta_{set\_H}$ ) and cooling ( $\theta_{set\_C}$ ) set point temperatures are obtained considering a constant dead band of  $\pm 2 \, ^\circ C$  from the  $\theta_{set\_id}$ .

The base ventilation flow rate needed at time step  $\tau_k$  to IAQ control ( $\dot{V}_{bs}$ ) can be calculated through the following piecewise-defined function

$$\dot{V}_{bs} = \begin{cases} f(w_{pig}) \cdot n_{pig} \cdot w_{pig} & w_{pig} < 50 \\ 0.17 \cdot w_{pig} \cdot n_{pig} & w_{pig} \geq 50 \end{cases} \quad (10)$$

with

$$f(w_{\text{pig}}) = (k_{\text{bs}_6} \cdot w_{\text{pig}}^6 + k_{\text{bs}_5} \cdot w_{\text{pig}}^5 + k_{\text{bs}_4} \cdot w_{\text{pig}}^4 + k_{\text{bs}_3} \cdot w_{\text{pig}}^3 + k_{\text{bs}_2} \cdot w_{\text{pig}}^2 + k_{\text{bs}_1} \cdot w_{\text{pig}} + k_{\text{bs}_0}) \left[ \frac{\text{m}^3}{\text{h}} \right] \quad (11)$$

where  $k_{\text{bs}_6} - k_{\text{bs}_0}$  are the polynomial regression coefficients obtained from [27] and reported in Table 2.

**Table 2** – Regression coefficients of Eqs. (9) and (11) used in this work.

Coefficient	Value	Unit of measurement
$k_{\text{set}_3}$	$-6.43424 \cdot 10^{-5}$	$^{\circ}\text{C kg}^{-3}$
$k_{\text{set}_2}$	$+1.12127 \cdot 10^{-2}$	$^{\circ}\text{C kg}^{-2}$
$k_{\text{set}_1}$	$-6.99575 \cdot 10^{-1}$	$^{\circ}\text{C kg}^{-1}$
$k_{\text{set}_0}$	$+32.55571$	$^{\circ}\text{C}$
$k_{\text{bs}_6}$	$+2.60378 \cdot 10^{-9}$	$\text{m}^3 \text{h}^{-1} \text{kg}^{-6}$
$k_{\text{bs}_5}$	$-4.87602 \cdot 10^{-7}$	$\text{m}^3 \text{h}^{-1} \text{kg}^{-5}$
$k_{\text{bs}_4}$	$+3.65480 \cdot 10^{-5}$	$\text{m}^3 \text{h}^{-1} \text{kg}^{-4}$
$k_{\text{bs}_3}$	$-1.40279 \cdot 10^{-3}$	$\text{m}^3 \text{h}^{-1} \text{kg}^{-3}$
$k_{\text{bs}_2}$	$+2.92192 \cdot 10^{-2}$	$\text{m}^3 \text{h}^{-1} \text{kg}^{-2}$
$k_{\text{bs}_1}$	$-3.18979 \cdot 10^{-1}$	$\text{m}^3 \text{h}^{-1} \text{kg}^{-1}$
$k_{\text{bs}_0}$	$+1.69046$	$\text{m}^3 \text{h}^{-1}$

Once defined all the needed boundary conditions for the considered simulation time step, the model solves the thermal balance, as described in the next section.

#### 4.2.3 Thermal balance module

In the present work, a customization of the sensible energy balance of the simple hourly method in compliance with ISO 13790 standard [51] is adopted. The simple hourly method adopts for the simulation an hourly time-step which is considered adequate in following the variation of the boundary conditions typical of pig houses. The reliability of the adopted simulation method was proved by previous works focused on civil buildings [52,53], livestock houses [54] and greenhouses [55]. The simple hourly method showed slight differences if compared with detailed dynamic energy simulation methods [46] or other hourly simulation methods [56].

The simple hourly method consists in the thermal-electrical analogy between the analysed building and an equivalent 5R1C electrical network (Figure 2), where five electrical resistances represent the heat transfer coefficients -namely  $H_{\text{ve}}$ ,  $H_{\text{tr\_fen}}$ ,  $H_{\text{tr\_em}}$ ,  $H_{\text{tr\_is}}$  and  $H_{\text{tr\_ms}}$ - and four nodes represent as many the lumped temperatures, namely  $\theta_{\text{air}_o}$ ,  $\theta_{\text{air}_i}$ ,  $\theta_s$  and  $\theta_m$ . In addition, four current sources represent as many heat flows, namely  $\phi_{\text{H/C\_nd}}$ ,  $\phi_{\text{ia}}$ ,  $\phi_{\text{st}}$  and  $\phi_m$ . The capacitor included in the equivalent electrical network represents the lumped fabric heat capacity of the building ( $C_m$ ).

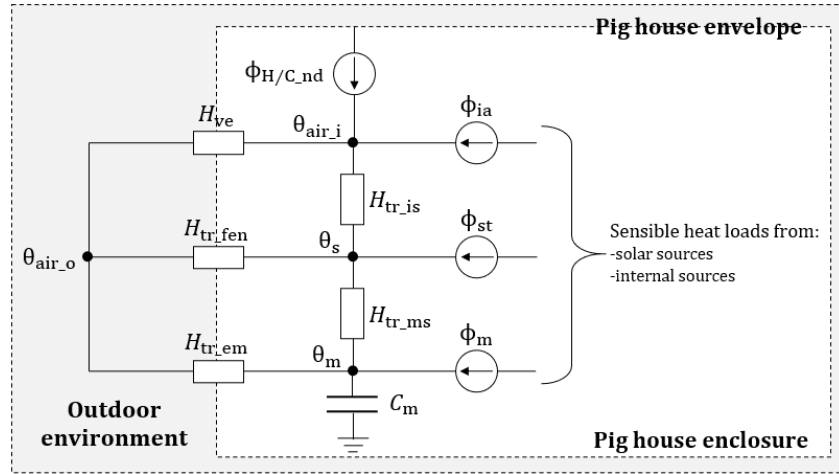


**Figure 2** - Schematization of the equivalent 5R1C electrical network implemented in the model for the simulation of the pig house thermal behaviour.

As shown by the schematization of Figure 2, the supplemental heating/cooling load ( $\phi_{H/C\_nd}$ ) needed to maintain the set point temperature is applied directly to the indoor air temperature node ( $\theta_{air\_i}$ ). This node is directly connected to the outdoor air temperature node ( $\theta_{air\_o}$ ) through the ventilation heat transfer coefficient ( $H_{ve}$ ). The node  $\theta_{air\_i}$  and the node of the internal surface temperature ( $\theta_s$ ) are connected between them through the heat transfer coefficient  $H_{tr\_is}$ . The simple hourly method simulates the heat exchange through the glazed and the opaque envelope in two different ways, as it follows. Regarding the glazed envelope, the model simulates that the heat is exchanged through the glazed surfaces directly to the outdoor environment. This heat transfer is function of the heat transfer coefficient  $H_{tr\_fen}$  and the difference between  $\theta_{air\_o}$  and  $\theta_s$ . The heat exchange through the glazed envelop occurs without any time delay since the glazed surfaces are considered without any heat capacity. By contrast, the heat storage phenomenon is considered when the heat exchange through the opaque envelope is calculated. To do so, the heat exchange is split into two components. First, the heat is exchanged between the surface of the opaque envelope and the building mass -at the temperature  $\theta_m$ - considering the heat transfer coefficient  $H_{tr\_ms}$ . Then, the heat is exchanged between the nodes  $\theta_m$  and  $\theta_{air\_o}$  considering the heat transfer coefficient  $H_{tr\_em}$  and the time delay caused by the heat storage phenomenon due to the building heat capacity ( $C_m$ ).

The heat flows that are considered in the simple hourly method, are calculated from the internal and solar heat loads. These heat loads are split into  $\phi_{ia}$  (convective flow),  $\phi_{st}$  (radiative flow) and  $\phi_m$  (radiative flow) and they are directly applied on the nodes  $\theta_{air\_i}$ ,  $\theta_s$  and  $\theta_m$ , respectively. The heat flow  $\phi_{H/C\_nd}$  is the supplemental heating/cooling load that is obtained once solved the thermal balance.

The analytical formulations for the calculation of each one of the previously presented terms can be found in paragraph C.3 of Annex C of ISO 13790 [51].

In the proposed model, the thermal balance is implemented to find the vector  $\vec{\theta}$ , that represents the values of the unknown temperatures of the problem that fulfil the thermal equilibrium of the system. Vector  $\vec{\theta}$  reads

$$\vec{\theta} = [\theta_{\text{air}_i} \quad \theta_s \quad \theta_m]^\theta \quad (12)$$

The value of the elements of  $\vec{\theta}$  can be determined solving the following set of constrained equation

$$A \cdot \vec{\theta} + B = 0 \quad (13)$$

with

$$A = \begin{bmatrix} -(H_{ve} + H_{tr_{is}}) & H_{tr_{is}} & 0 \\ H_{tr_{is}} & -(H_{tr_{is}} + H_{tr_{fen}} + H_{tr_{ms}}) & H_{tr_{ms}} \\ 0 & H_{tr_{ms}} & -(H_{tr_{ms}} + H_{tr_{em}} + 3.6^{-1} \cdot C_m) \end{bmatrix} \quad (14)$$

and

$$B = \begin{bmatrix} H_{ve} \cdot \theta_{\text{air}_o} + \phi_{ia}(\theta_{\text{air}_i}) + \phi_{H/C_{nc}}(\cdot) \\ H_{tr_{fen}} \cdot \theta_{\text{air}_o} + \phi_{st} \\ H_{tr_{fen}} \cdot \theta_{\text{air}_o} + \phi_m + 3.6^{-1} \cdot C_m \cdot \theta_{m,k-1} \end{bmatrix} \quad (15)$$

Please note that the heating or cooling thermal flow  $\phi_{H/C_{nc}}(\cdot)$  is defined as

$$\phi_{H/C_{nc}}(\cdot) \begin{cases} < 0 & \text{if } \theta_{\text{air}_i} > \theta_{\text{set}_C} \\ = 0 & \text{if } \theta_{\text{set}_H} \leq \theta_{\text{air}_i} \leq \theta_{\text{set}_C} \\ > 0 & \text{if } \theta_{\text{air}_i} < \theta_{\text{set}_C} \end{cases} \quad (16)$$

since  $\theta_{\text{air}_i}$  is a constrained variable that could vary in the range  $[\theta_{\text{set}_H} \quad \theta_{\text{set}_C}]$ .

At each time step of the simulation, the term  $H_{ve}$  present in matrix B is calculated at as

$$H_{ve} = \frac{\rho_{\text{air}} \cdot c_{\text{air}} \cdot \dot{V}_{\text{act}}}{3.6 \cdot 10^3} \quad \left[ \frac{\text{W}}{\text{K}} \right] \quad (17)$$

where  $\rho_{\text{air}}$  is the volumetric mass density of the ventilation air ( $\text{kg m}^{-3}$ ) and  $c_{\text{air}}$  is the specific heat capacity of ventilation air ( $\text{J kg}^{-1} \text{K}^{-1}$ ). The term  $\dot{V}_{\text{act}}$  is the actual ventilation air flow rate ( $\text{m}^3 \text{h}^{-1}$ ) of the pig house which value depends on the boundary conditions, as schematized in Figure 3. At each simulation time step, in fact, three cases can occur. In the times steps in which pigs are not present inside the house -e.g. sanitary empty periods-,  $\dot{V}_{\text{act}}$  is equal to  $\dot{V}_{\text{min}}$  (case A) that is a minimum ventilation air flow rate that is maintained inside the house to guarantee a safety environment for workers. The value of  $\dot{V}_{\text{min}}$  is an input data of the model. If pigs are

present in the house, two different cases may occur depending on  $\theta_{\text{air}_i}$  value at the considered time step. If  $\theta_{\text{air}_i} \leq \theta_{\text{set}_C}$ , ventilation is just needed to control IAQ (case B). In this case,  $\dot{V}_{\text{act}}$  is equal to  $\dot{V}_{\text{bs}}$  that is calculated according to Eq. (10). The last case presented in Figure 3 (case C) regards those time steps in which pigs are present inside the house and  $\theta_{\text{air}_i} \geq \theta_{\text{set}_C}$ , meaning that a theoretical cooling load is needed. Since mechanical cooling is usually not present in pig houses, the theoretical cooling load estimated by the model ( $\phi_{C\_nd}$ ) is converted in an equivalent cooling ventilation flow rate ( $\dot{V}_{\text{cool}}$ ). Therefore, in those time steps,  $\dot{V}_{\text{act}}$  is equal to  $\dot{V}_{\text{cool}}$  that reads

$$\dot{V}_{\text{cool}} = \min \left[ \frac{|\phi_{C\_nd}|}{(\theta_{\text{set}_C} - \theta_{\text{air}_o})} \cdot \frac{3.6 \cdot 10^3}{\rho_{\text{air}} \cdot c_{\text{air}}}; \dot{V}_{\text{max}} \right] \left[ \frac{\text{m}^3}{\text{h}} \right] \quad (18)$$

where  $\dot{V}_{\text{max}}$  is the maximum ventilation flow rate that is installed in the growing-finishing pig house.

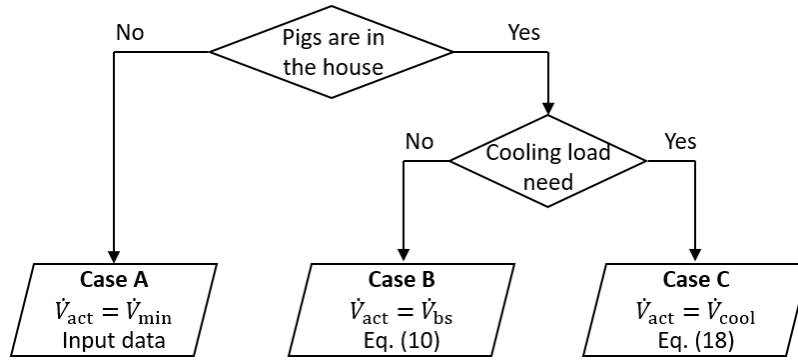


**Figure 3** - Flow chart for the calculation of the actual ventilation flow rate ( $\dot{V}_{\text{act}}$ ) adopted in the presented energy simulation model.

Once calculated  $\dot{V}_{\text{act}}$ , the solution of Eq. (13) at time instant  $k$  can be numerically computed solving the problem

$$\vec{\theta}^{(k)} = A^{-1} \cdot (-B) \quad (19)$$

When  $\theta_{\text{air}_i}$  is in free-floating conditions ( $\theta_{\text{set}_H} \leq \theta_{\text{air}_i} \leq \theta_{\text{set}_C}$ ), matrix  $A^{-1}$  cannot be computed and the problem is solved using the Runge-Kutta solver. The main outputs that are obtained from the solution of the thermal balance are the heating ( $\phi_{H\_nd}$ ) or the cooling ( $\phi_{C\_nd}$ ) loads -when air is not in free-floating conditions- and  $\theta_{\text{air}_i}$ .

#### 4.2.4 Moisture balance module

At each simulation time step, the moisture balance of the pig house is solved to find the indoor air humidity ratio ( $x_{\text{air}_i}$ ) and the hourly value of  $RH_i$ . Knowing the vapour production from internal sources ( $\dot{m}_i$ ) calculated through Eq. (7), the water vapour balance in dynamic conditions can be described through the following ordinary pure-time differential equation

$$\frac{dx_{air,i}}{dt} \cdot V \cdot \rho_{air} = \dot{m}_i + \dot{V}_{act} \cdot \rho_{air} \cdot (x_{air,o} - x_{air,i}) \quad \left[ \frac{kg_{vap}}{h} \right] \quad (20)$$

where  $V$  is the pig house net volume ( $m^3$ ),  $\rho_{air}$  is the volumetric mass density of air ( $kg\ m^{-3}$ ),  $\dot{V}_{act}$  is the actual ventilation flow rate ( $m^3\ h^{-1}$ ) calculated in the previous module and  $x_{air,o}$  is the outdoor air humidity ratio ( $kg_{vap}\ kg_{air}^{-1}$ ). The solution of the previous equation is

$$x_{air,i}(\tau_k + \Delta\tau) = x_{air,o} + \frac{(\dot{m}_i)}{\dot{V}_{act} \rho_{air}} + \left[ x_{air,i}(\tau_k) - x_{air,o} - \frac{(\dot{m}_i)}{\dot{V}_{act} \rho_{air}} \right] \cdot e^{-\left(\frac{\dot{V}_{act}}{V}\right) \cdot \Delta\tau} \quad \left[ \frac{kg_{vap}}{kg} \right] \quad (21)$$

where  $\Delta\tau$  is the duration of the time step.

The balance is solved at each time step of simulation to find  $x_{air,i}$ . knowing  $x_{air,i}$  and  $\theta_{air,i}$ , the hourly value of  $RH_i$  is obtained through psychrometric formulations.

#### 4.2.5 System efficiency module

At the end of the calculation loop, the energy simulation model estimates the overall thermal ( $E_{th}$ ) and electrical ( $E_{el}$ ) energy consumption due to climate control, considering the efficiency of both the heating and ventilation systems.

The overall thermal energy consumption  $E_{th}$  is calculated as

$$E_{th} = \sum_{k=1}^{n_k} \left( \frac{\phi_{H,nd,k} \cdot \Delta\tau}{\eta_H \cdot 10^3} \right) \quad [kWh] \quad (22)$$

where  $\phi_{H,nd,k}$  is the supplemental heating load provided ad each time step  $k$  (in  $W$ ),  $\eta_H$  is the dimensionless global efficiency of the heating system installed in the pig house and  $n_k$  is the number of considered time steps of the simulation.

The electrical energy consumption due to ventilation  $E_{el}$ , is calculated considering the presence of fixed angular speed fans that deals with both  $IAQ$  control and cooling ventilation. Fixed angular speed fans cannot regulate their propeller speed and, consequently, the airflow provided by the fan ( $\dot{V}_{fan}$ ) is only function of the static pressure difference between inside and outside the pig house ( $\Delta p_{st}$ ). In agricultural applications, such as poultry and pig houses,  $\Delta p_{st}$  is usually around 20-30 Pa and climate control system manages the opening of the air inlets to maintain  $\Delta p_{st}$  constant during the day [57]. At each  $k$ -th time step, the effective airflow of a fixed speed fan  $\dot{V}_{fan,j}$  can be calculated as

$$\dot{V}_{fan,k} = k_{fan,2} \cdot \Delta p_{st,k}^2 + k_{fan,1} \cdot \Delta p_{st,k} + k_{fan,0} \quad \left[ \frac{m^3}{h} \right] \quad (23)$$

where  $k_{fan,2}$  -  $k_{fan,0}$  are regression coefficients obtainable from the technical datasheet of the fan model.

Similarly, the electrical energy consumption of a fixed angular speed fan varies according to the Specific Fan Performance (*SFP*) as a function of  $\Delta p_{st}$ . At each  $k$ -th time step,  $SFP_k$  reads

$$SFP_k = k_{SFP_2} \cdot \Delta p_{st,k}^2 + k_{SFP_1} \cdot \Delta p_{st,k} + k_{SFP_0} \quad \left[ \frac{\text{m}^3}{\text{Wh}} \right] \quad (24)$$

where  $k_{SFP_2} - k_{SFP_0}$  are regression coefficients obtainable from the technical datasheet of the fan model.

The overall electrical energy consumption due to ventilation  $E_{el}$  is then calculated as

$$E_{el} = \sum_{k=1}^{n_k} \left( \frac{\dot{V}_{act,k}}{SFP_k} \cdot \Delta \tau \right) \cdot 10^{-3} \quad [\text{kWh}] \quad (25)$$

where  $\dot{V}_{act,k}$  and  $SFP_k$  are the effective ventilation flow and the Specific Fan Performance calculated at the  $k$ -th time step, respectively.

## 5 Pig house energy model: validation

Validation can be defined as the process of confirming that the model predictions adequately represent measured physical phenomena [58]. The developed energy simulation model was validated against real monitored data to assess its reliability in estimating the indoor climate conditions and the energy consumption for climate control. For this purpose, a selected case-study was monitored during 31 days to acquire the needed dataset that was then compared with the results of a simulation tailored on the features of the case study. The acquired data and the simulation results were used to calculate goodness-of-fit indexes that are then compared to threshold values established by international guidelines and protocols.

### 5.1 Case study description and modelling specifications

The monitored growing-finishing pig house (Figure 4) is part of a larger farmstead located in Northwestern Italy. The monitored building is 17.8 m long and 15.68 m width, as visible from the schematization reported in Figure 5. The height from the floor to the ridge is 3.95 m. Inside, the house is divided in pens and has a partially slatted floor that separates the enclosure from the pit -1.4 m deep- where manure is collected. The useful floor area of the house is around 280 m<sup>2</sup> and the volume, excluding the pit, is around 1,030 m<sup>3</sup>.



**Figure 4** – External (a) and internal (b) views of the monitored pig house.

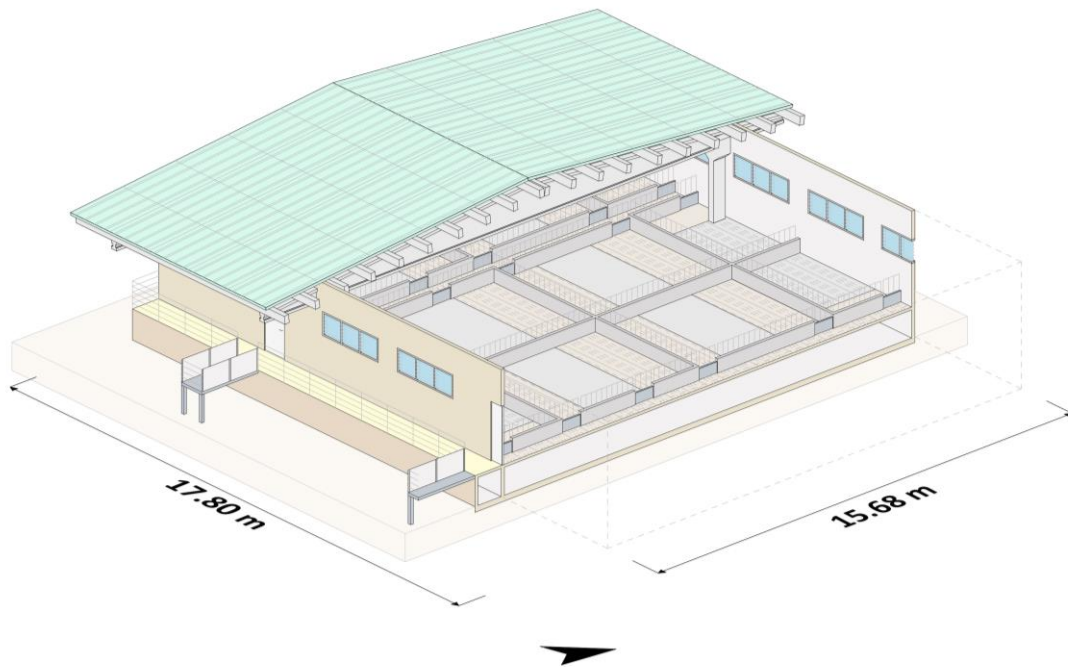


**Figure 5** – Schematization of the monitored growing-finishing pig house.

The monitored building has a reinforced concrete structure with prefabricated beams and pillars. The walls are composed by piled hollow blocks and the roof is composed by prefabricated sandwich panels. The air inlets are polycarbonate hollow sheets with metal frames. The thermal transmittances ( $U - value$ ) of the building elements of the envelope are presented in Table 3, where their internal aerial heat capacities ( $\kappa_i$ ) are also presented. As it is visible from the table, all the envelope components are characterized by high  $U - value$ . The only exception is the roof since it is the only envelope element with a thermal insulation layer. The  $\kappa_i$  values presented in Table 3 are needed for the calculation of the total building fabric



heat capacity ( $C_m$ ) of the pig house. For this purpose, the presence of internal structural elements was considered.

**Table 3** – Stationary thermal transmittance ( $U$  – value) and internal aerial heat capacities ( $\kappa_i$ ) of the components of the building envelope of the considered case study.

Envelope component	$U$ – value [W m <sup>-2</sup> K <sup>-1</sup> ]	$\kappa_i$ [kJ m <sup>-2</sup> K <sup>-1</sup> ]
Walls	2.18	55.8
Roof	0.64	3.8
Partially slatted floor	2.88	60.2
Air inlets	3.40	-

The ventilation system of the analysed growing-finishing pig house is composed by three exhaust fans placed at the pit level that are used to control both IAQ and  $\theta_{air,i}$ . Each 6-blade fan -0.5 m of diameter- has 0.43 kW of mechanical power and its maximum airflow in free delivery conditions ( $\Delta p_{st} = 0$  Pa) is around 6,500 m<sup>3</sup> h<sup>-1</sup>. The fans of the monitored pig house were characterized as specified in Eqs. (23) and (24) through a polynomial regression on data reported in their technical datasheet. The obtained coefficients are reported in Table 4. The installed fans are controlled by a climate control unit that also manages the inlet opening to maintain a constant  $\Delta p_{st}$  of 20 Pa during the production cycle. The heating systems is composed by two portable diesel oil air heaters of 67 kW of heating capacity each one that are placed inside the house only during the cool season.

**Table 4** – Coefficients for fan characterization (Eqs. (24) and (25)).

Coefficient	Value	Unit of measurement
$k_{fan,2}$	-5.8796·10 <sup>-2</sup>	m <sup>3</sup> h <sup>-1</sup> Pa <sup>-2</sup>
$k_{fan,1}$	-25.7989	m <sup>3</sup> h <sup>-1</sup> Pa <sup>-1</sup>
$k_{fan,0}$	+6,496.24	m <sup>3</sup> h <sup>-1</sup>
$k_{SFP,2}$	-1.7888·10 <sup>-3</sup>	m <sup>3</sup> Wh <sup>-1</sup> Pa <sup>-2</sup>
$k_{SFP,1}$	-6.3776·10 <sup>-2</sup>	m <sup>3</sup> Wh <sup>-1</sup> Pa <sup>-1</sup>
$k_{SFP,0}$	+11.14	m <sup>3</sup> Wh <sup>-1</sup>

## 5.2 Monitoring campaign description

The indoor climate conditions and the electrical energy consumption for ventilation of the considered pig house were monitored from July 1<sup>st</sup> to 31<sup>st</sup> (744 hours), through the installation of an *ad-hoc* sensor network. This period was only part of a longer production cycle that took place in the warm season, from March 22<sup>nd</sup> to August 25<sup>th</sup> (156 days). During this cycle, 155 pigs were reared until the final live weight of about 173 kg. This final live weight is typical on the Italian market where heavy pigs are farmed for cured meat production, such as dry-cured ham.

The coefficients for simulating pig growth through Eq. (1) - $W_{pig}$ ,  $\delta_{pig}$  and  $a_{pig\_max}$ - were obtained by fitting the Gompertz function on growing data provided by the farmer and they are presented in Table 4. In Figure 6, trend of pig growth -estimated by Eq. (1)- during the considered production cycle is presented. The monitoring period (July 1<sup>st</sup> to August 6<sup>th</sup>) is highlighted with a green background. The graph shows that at the beginning of the monitoring period pig age was 190 days while at the end of it their age was 227 days. During the monitoring period, pig live weight increases approximatively from 130 kg to 161 kg, meaning an average daily increase of 0.84 kg per day.

**Table 4** – Coefficients for pig growth simulation through Eq. (1).

Coefficient	Value
$W_{pig}$	218.16 kg
$\delta_{pig}$	0.0142 days <sup>-1</sup>
$a_{pig\_max}$	143.10 days

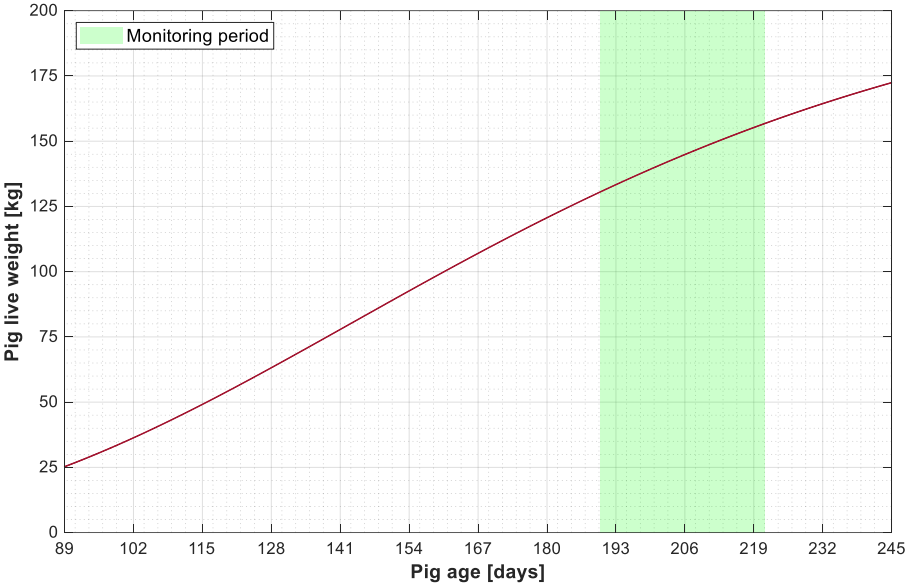


**Figure 6** – Trend of pig growth during the production cycle. The monitoring period is highlighted with a green background.

The indoor climate conditions were measured and logged using four data loggers (Figure 7a) that embed a thermistor for the measurement of  $\theta_{air,i}$  (accuracy:  $\pm 0.21$  °C) and a humistors for the measurement of  $RH_i$  (accuracy:  $\pm 2.5\%$ ). All the installed devices adopted a *USB* communication protocol and they were installed evenly spaced inside the house on existing supports. With this configuration, four measurement points for  $\theta_{air,i}$  and  $RH_i$  were set inside the monitored growing-finishing pig house. All the data loggers were set with a 10-minute acquisition time step. At each acquisition time step, the data acquired by the sensors were

averaged between them to have single values of  $\theta_{\text{air}_i}$  and of  $RH_i$  that can be considered representative of the entire enclosure. Then, the obtained 10-minute values of  $\theta_{\text{air}_i}$  and  $RH_i$  were averaged on an hourly time basis to be comparable with the numerical model outputs.

The values of  $\theta_{\text{air}_o}$  and  $RH_o$  were obtained by arranging a portable data logger with an embedded humistor and thermistor outside the pig house, shielded from solar radiation. The obtained outdoor weather conditions were integrated using the hourly data from a third-part weather station (Regional Agency for the Protection of the Environment of Piemonte, ARPA Piemonte) that also provided the total solar radiation on the horizontal plane.

The performed monitoring campaign was aimed also at monitoring the electrical power absorbed by the fans. To do so, an AC kilowatt transducer (accuracy:  $\pm 1\%$ ) that incorporates three split-core AC current sensors and three voltage leads (Figure 7a) was installed in the breaker electrical panel of the house. The datalogger connected to the AC kilowatt transducer was set with a 10-seconds logging time step. The 10-second electrical power data were integrated in time to obtain the daily electrical energy consumption for ventilation.

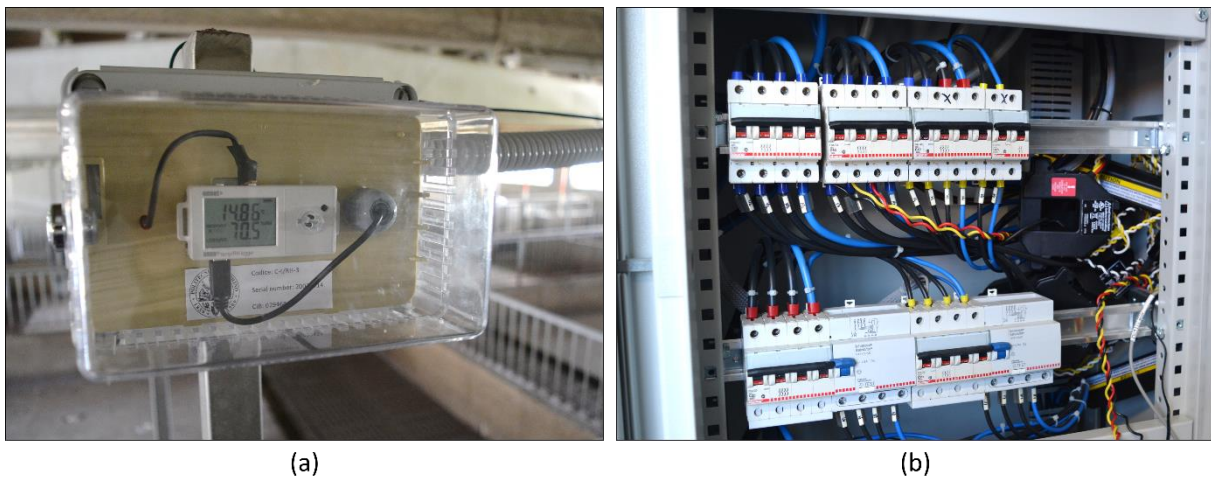


**Figure 7** – Data logger with embedded thermistor and humistor (a) and AC kilowatt transducer with three split-core AC current sensors (b).

### 5.2.1 Focus on monitored data

The monitored data of  $\theta_{\text{air}_i}$  and  $RH_i$  can be used to give an overview of the pig heat stress risk during the monitored period. When pigs are exposed to high  $\theta_{\text{air}_i}$  and  $RH_i$  their capacity to dissipate metabolic heat is compromised, they decrease the feed intake and may face serious health problems. The level of heat stress risk of farmed pigs can be assessed by evaluating the combined effect of  $\theta_{\text{air}_i}$  and  $RH_i$  considering threshold values provided in literature, as done in the scatterplot of Figure 8. The cartesian coordinates of each point of the scatter plot are  $\theta_{\text{air}_i}$  ( $x$ -axis) and  $RH_i$  ( $y$ -axis) values are calculated as the average among all the measurements

performed at each 10-minute time step. In the plot, the three risky zones for heat stress reported in [59] are presented using different background colours. In alert zone, yellow background, pig may start to suffer from heat stress. For this reason, ventilation should be increased and pigs should be monitored to detect possible signs of heat stress, such as panting. In danger zone, orange background, additional cooling systems should be adopted, such as water spraying or misting. In the emergency zone, red background, pigs are suffering from heat stress and their activity should be reduced by withdrawing feed and reducing light level.

The scatter plot of Figure 8 shows that the analysed pig house was characterized by considerably high values of  $\theta_{air,i}$  and  $RH_i$  during the monitored period. The values of  $\theta_{air,i}$ , in fact, varied approximately between 24 and 34 °C, values that are significantly far from  $\theta_{set,id}$  that was calculated through Eq. (8). This reflects on the heat stress risk. The scatter plot, in fact, shows that pigs were in danger and emergency situations during almost all the monitored period, a situation that was also favoured by the high values of  $RH_i$  that ranged mainly between 50 and 70% during the monitored period. Similar high  $\theta_{air,i}$  and  $RH_i$  values may would have influenced the pig mortality that was around 4% during the monitored production cycle.

The performed analysis shows the importance of adopting further cooling strategies, such as the ones proposed by Panagakis & Axaopoulos [44], to decrease pig heat stress during the warm season. This is of the foremost importance considering that global climate change is expected to increase the frequency of extreme events -i.e., number of hot days and of heat waves- in temperate areas, increasing the negative impact of heat stress on livestock production [60].

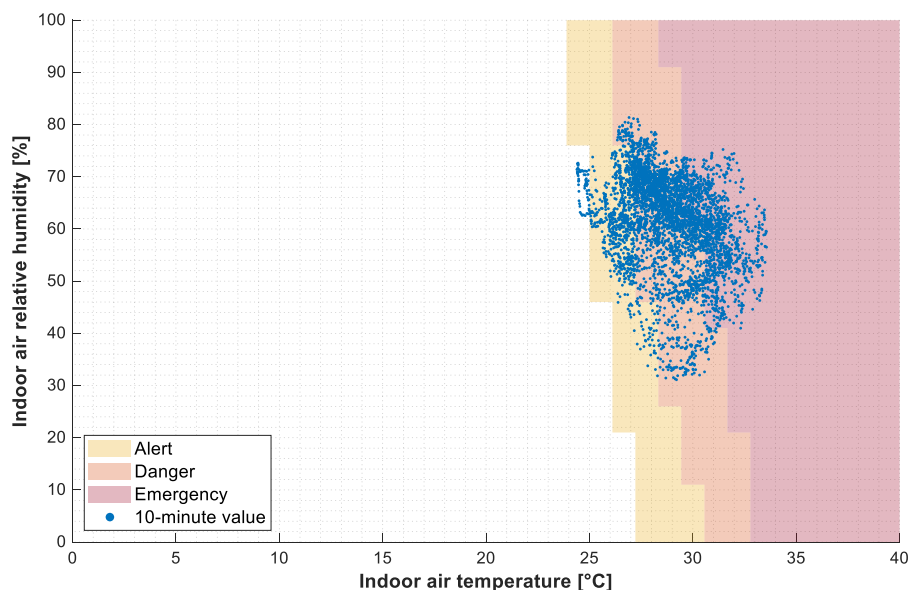


**Figure 8** – Indoor climate conditions of air temperature and relative humidity during the monitored period and heat stress risky zones.

### 5.3 Validation results

The acquired dataset is here used to evaluate the reliability of the model. In Figure 9, the monitored trends of  $\theta_{\text{air}_i}$  and  $RH_i$  are presented with an hourly time basis together with the trends of  $\theta_{\text{air}_i}$  and  $RH_i$  estimated by the model. The trends of the monitored  $\theta_{\text{air}_o}$  and  $RH_o$  are also presented in the figure. The presented graph shows that, during the monitored period,  $\theta_{\text{air}_o}$  was considerably high, with values that often exceed 30 °C during daytime. During nighttime,  $\theta_{\text{air}_o}$  decreased considerably, especially during the first days of the monitoring period, when it reached a minimum of 14 °C. In the following days,  $\theta_{\text{air}_o}$  was almost always higher than 20 °C. These high values of  $\theta_{\text{air}_o}$ , explain the higher values of monitored  $\theta_{\text{air}_i}$  that, as stated in the previous section, may be detrimental for pig health.

The chart shows that the simulated and monitored trends of  $\theta_{\text{air}_i}$  are quite similar between them during the entire analysed period. The main difference that can be noticed between the considered trends regards the peaks that can be observed during daytime. The energy simulation model, in fact, estimates maximum  $\theta_{\text{air}_i}$  during daytime that are slightly higher than the monitored ones. A similar pattern can be observed also for the minimum  $\theta_{\text{air}_i}$  values estimated during nighttime since the model estimates lower  $\theta_{\text{air}_i}$  than the monitored ones. These differences are more evident, for example, in the period between July 23<sup>rd</sup> and 28<sup>th</sup> and they can be attributable to a slight underestimation of the building fabric heat capacity ( $C_m$ ).

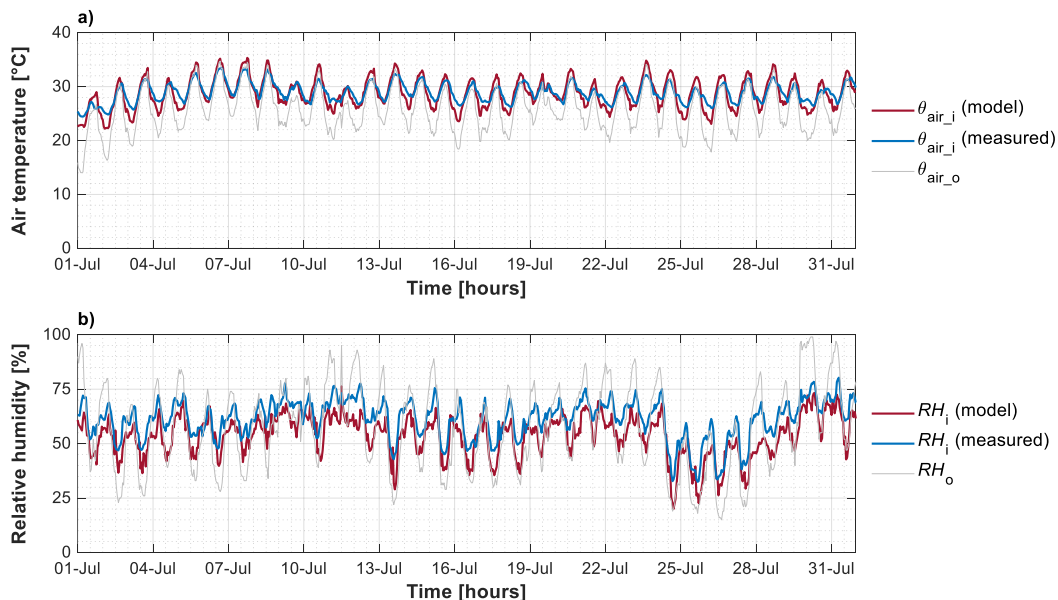


**Figure 9** – Comparison between simulated and measured values of hourly indoor air temperature ( $\theta_{\text{air}_i}$ ) and relative humidity ( $RH_i$ ). Outdoor monitored values of air temperature ( $\theta_{\text{air}_o}$ ) and relative humidity ( $RH_o$ ) are presented.

Figure 9 makes it also possible the comparison between the monitored and simulated trends of  $RH_i$ . The model estimates with a good approximation the trend of the monitored  $RH_i$ , but an underestimation of  $RH_i$  stands out. Part of this difference could be due to the previously presented deviation between the estimated and monitored  $\theta_{air\_i}$  since -as it is well known-  $RH_i$  is function of the saturated water vapour pressure and, in turn, of  $\theta_{air\_i}$ . Therefore, the differences between  $\theta_{air\_i}$  trends reflect on the considered  $RH_i$  trends. The deviation between the estimated and the monitored  $RH_i$  trends can be also attributable to an underestimation of the water vapour emission from internal sources. Even though the formulations that are used in this work estimate the vapour emissions at house level including feed, waterers and manure, the vapour emission from the pit may be underestimated since, in the analysed pig house, manure is flushed only at the end of the production cycle. In addition, the monitored period was characterized by high values of  $\theta_{air\_o}$  that may have contributed to increase the moisture production from manure. Even though pit ventilation was adopted in the considered case study, air stagnation pockets may have been present favouring the mass transportation from pit to enclosure. Further works may deepen the analysis of this specific issue with the aim of understanding the dynamics of ventilation air and contaminants between the enclosure and the pit adopting, for example, zonal or *CFD* models [61].

As stated before, the reliability of the presented energy simulation model is numerically evaluated by comparing statistical goodness-of-fit indexes -calculated between the measured and simulated data- with the threshold values established by the following international standards and protocols:

- Guideline 14 of the American Society of Heating, Refrigerating and Air-Conditioning Engineers (ASHRAE) [62];
- International Performance Measurements and Verification Protocol (IPMVP) [63];
- Federal Energy Management Program (FEMP) Measurements and Verification guidelines [64].

The considered goodness-of-fit indexes are the Mean Bias Error (*MBE*) and the Coefficient of variation of the Root Mean Square Error (*CvRMSE*).

The Mean Bias Error (*MBE*) reads

$$MBE = \frac{\sum_{j=1}^{n_{set}} (\tilde{\chi}_j - \chi_j)}{\sum_{j=1}^{n_{set}} \tilde{\chi}_j} \cdot 100 \quad [\%] \quad (26)$$

where  $\chi_j$  and  $\tilde{\chi}_j$  are the simulated and measured values at the hourly time-step  $j$ , respectively, while  $n_{set}$  is the cardinality of the considered set of data (888 hourly values).

The other considered goodness-of-fit- index,  $CvRMSE$ , reads

$$Cv(RMSE) = \frac{RMSE}{\left(\sum_{j=1}^{n_{set}} \tilde{\chi}_j\right) \cdot \frac{1}{n_{set}}} \cdot 100 \quad [\%] \quad (27)$$

where  $RMSE$  is the Root Mean Square Error that is calculated as

$$RMSE = \sqrt{\frac{\sum_{j=1}^{n_{set}} (\chi_j - \tilde{\chi}_j)^2}{n_{set}}} \quad (28)$$

which unit of measurement is the same of  $\chi_j$  and  $\tilde{\chi}_j$ .

In Table 5, the goodness-of-fit indexes calculated for  $\theta_{air,i}$  and  $RH_i$  are presented together with their thresholds from ASHRAE [62], IPMVP [63] and FEMP [64]. Even though  $RMSE$  has not a threshold value, it is reported in the table since it a good indicator of the extent of the error between the estimated and the monitored trends. Table 5 confirms what it was stated comparing the estimated and monitored trends of Figure 9. The model, in fact, is reliable for the estimation of  $\theta_{air,i}$ . The  $RMSE$  between the estimated and monitored trends over the 744 hours of simulation is 1.42 °C. The model estimation of  $\theta_{air,i}$  widely respects the established threshold values, even the more restrictive of IPMVP [63]. The  $MBE$ , in fact, is 0.72%, a value considerably lower than the ASHRAE [62] and FEMP [64] threshold ( $\pm 10\%$ ) and IPMVP [63] threshold ( $\pm 5\%$ ).

The reliability of the model regarding  $RH_i$  can be considered good, even though the  $MBE$  value (12.19%) is slightly higher than the established thresholds ( $\pm 10\%$  and  $\pm 5\%$ ), as visible in Table 5. Nevertheless, the model estimation is characterized by a low  $RMSE$  of 8.79%, over the entire period. The model respects all the thresholds for the  $Cv(RMSE)$ . The calculated  $Cv(RMSE)$ , in fact, is 14.38%, while the most restrictive threshold (IPMVP [63]) is 20%.

**Table 5** – Goodness-of-fit indexes with their thresholds for indoor air temperature ( $\theta_{air,i}$ ) and relative humidity ( $RH_i$ ).

Parameter	Goodness-of-fit index	Value	Threshold values (hourly validation)		
			ASHRAE [62]	IPMVP [63]	FEMP [64]
$\theta_{air,i}$	$MBE^a$	0.72%	$\pm 10\%$	$\pm 5\%$	$\pm 10\%$
	$Cv(RMSE)^b$	4.91%	30%	20%	30%
	$RMSE^c$	1.42 °C	-	-	-
$RH_i$	$MBE$	12.08%	$\pm 10\%$	$\pm 5\%$	$\pm 10\%$
	$Cv(RMSE)$	14.38%	30%	20%	30%
	$RMSE$	8.79%	-	-	-

<sup>a</sup> Mean Bias Error

<sup>b</sup> Coefficient of Variation of the Root Mean Square Error

The last evaluation of model reliability regards the estimation of the electrical energy consumption for ventilation. In Figure 10, the monitored and estimated electrical energy consumption for ventilation of the analysed case study are compared in a bar chart. The graph shows that the daily electrical energy consumption of the monitored growing-finishing pig house was between around 28 and 44 kWh during the monitored period. This energy consumption shows that fans operate during most of the time to guarantee adequate  $\theta_{\text{air}_i}$  values in a period in which  $\theta_{\text{air}_o}$  was considerably high, as shown in Figure 9. The bar chart shows that the model correctly estimates the electrical energy consumption with few exceptions. The main deviation between the estimated and the monitored electrical energy consumption is on July 19<sup>th</sup>, where the monitored electrical energy consumption was around 28 kWh while the estimated one was around 44 kWh. This difference may be attributable to a manual deactivation of the ventilation system by farm workers to perform specific tasks inside the house, a hypothesis that was not possible to verify with certainty.

The total energy consumption that was acquired during the entire monitoring campaign was around 1,329 kWh of electrical energy, while the model estimated 1,361 kWh. It means that the energy simulation model overestimates the energy consumption over the entire period by less than 3% (32 kWh), an error that can be considered acceptable for the purpose of the present work.

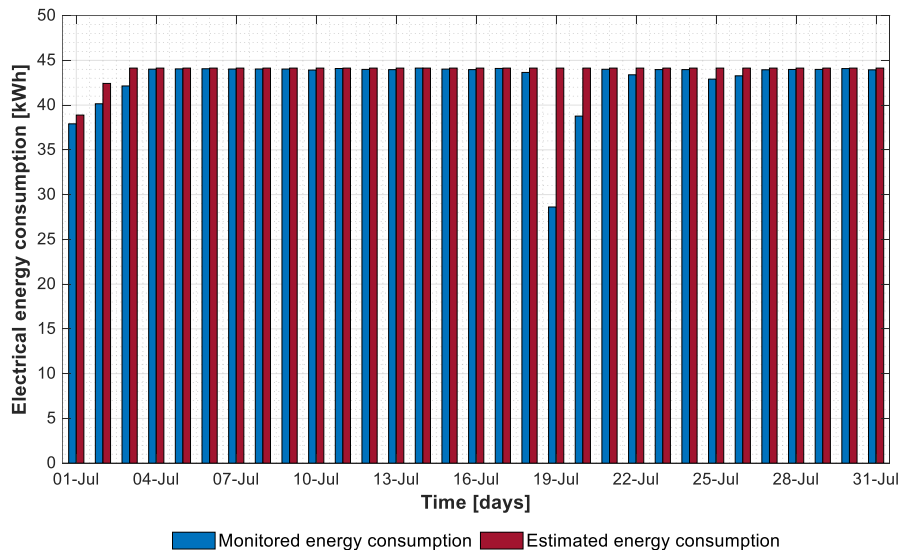


**Figure 10** – Comparison between the daily monitored and estimated electrical energy consumption for ventilation.

## 6 Model application



The presented dynamic thermal model is full of potentiality for investigating energy-related topics of intensive pig farming in climate-controlled pig houses. This is because the presented model enhances the simulation of pig houses in standardized conditions, considering different geographical contexts, different climate control equipment and different farming features.

To give an overview about the several opportunities that this model could provide to stakeholders, an example of application is provided by simulating the same growing-fattening pig house presented in section 5.1. For this purpose, six different scenarios characterized by specific geographical contexts, are considered (Table 6). Each scenario represents a pig production cycle of 135 days carried out during the cool and the warm season. At the end of the production cycle, pigs reach a final live weight of around 160 kg. The considered countries - Italy, Spain, and Germany- are chosen since they are the most important European producers of pigs for cured meat production, as reported in a survey of the European Commission [65]. A reference city is selected for each geographical context and its Typical Meteorological Year (TMY) is adopted for performing the simulation. As visible from Table 6, each scenario is characterized by quite different values of average hourly  $\theta_{air_o}$  during the production cycle, being the minimum value 2.4 °C from DE-C scenario and the maximum one 22.2 °C from ES-W scenario.

**Table 6** – main features of the considered simulation scenarios.

Scenario	Season	Geographical context (reference city)	Average hourly $\theta_{air_o}$
IT-C	Cool season <sup>a</sup>	Italy (Bologna)	3.3 °C
IT-W	Warm season <sup>b</sup>	Italy (Bologna)	20.2 °C
ES-C	Cool season	Spain (Barcelona)	10.0 °C
ES-W	Warm season	Spain (Barcelona)	22.2 °C
DE-C	Cool season	Germany (Bremen)	2.4 °C
DE-W	Warm season	Germany (Bremen)	15.3 °C

<sup>a</sup> November 1<sup>st</sup> – March 16<sup>th</sup>

<sup>b</sup> June 1<sup>st</sup> – October 14<sup>th</sup>

The first assessment that can be carried out through the energy simulation model is an estimation of the differences concerning heat stress risk with the same procedure adopted in section 5.2.1. The cartesian coordinates of each point of the scatter plot of Figure 11 are the hourly values of  $\theta_{air_i}$  and  $RH_i$  simulated for the analysed scenarios. From the graph, it is evident that scenarios IT-C and ES-C are the ones characterized by the highest risk of heat stress since animals are in alert, danger, or emergency situations during several hours of the production cycles. By contrast, heat stress seems to be a minor issue in DE-W scenario since the farmed pigs are in alert or danger situation during only few hours of the production cycle.

This difference between the scenarios is attributable to the different  $\theta_{\text{air}_o}$  values during the production cycles, as reported in Table 6. During cool season, heat stress is not an issue in none of the considered scenarios, namely IT-C, ES-C and DE-C. Nevertheless, the results of the simulations highlight that IT-C and DE-C scenarios could be characterized by significant humidity problems since  $RH_i$  is often over 70%. These humidity problems may lead to an increase of heating energy consumption, as reported by Fernandez et al. [66]. The presented model, hence, can be used to numerically estimate the needed increase of ventilation air flow rate to decrease  $RH_i$  considering the consequent increase of electrical energy consumption due to fan activation and thermal energy consumption due to the increased heat losses. In this way, it could be possible to find a trade-off between improving the indoor climate conditions for pig farming and decreasing the energy consumption for climate control of the pig house. By contrast, the humidity problem is not present in scenario ES-W, as visible from Figure 11b). The high  $\theta_{\text{air}_o}$  typical of this scenario, in fact, entails a higher ventilation flow rate to decrease  $\theta_{\text{air}_i}$  that entails a consequent decrease of  $RH_i$  too.

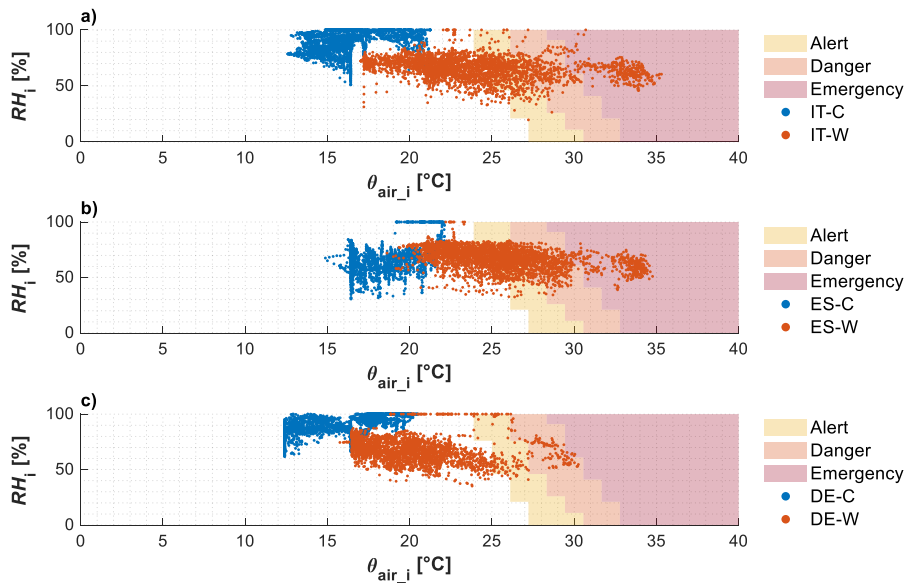


**Figure 11** – Hourly indoor climate conditions of air temperature and relative humidity for the considered scenarios. a) Italy: cool (IT-C) and warm (IT-W) seasons; b) Spain: cool (ES-C) and warm (ES-W) seasons; c) Germany: cool (DE-C) and warm (DE-W) seasons.

The different outdoor climate conditions in which the production cycles take place have also important consequences on the energy consumption for maintaining adequate  $\theta_{\text{air}_i}$  values inside the analysed pig house, as visible from Table 7. In the table, the thermal energy consumption for supplemental heating ( $E_{\text{th}}$ ) and the electrical energy consumption for ventilation ( $E_{\text{el}}$ ) are shown for each one of the considered scenarios. Supplemental heating can

be considered a minor issue in almost all the considered scenarios. No supplemental heating, in fact, is needed in the scenarios that consider the warm season -IT-W and ES-W- with the only exception of DE-W, where a slight value of  $E_{th}$  is estimated. The situation in the scenarios that consider the cool season -IT-C, ES-C and DE-C- is quite different. In ES-C scenario, the mild outdoor weather conditions of the considered area of Spain and the pig thermal emissions are enough to maintain adequate value of  $\theta_{air,i}$  without using mechanical heating systems. Therefore no  $E_{th}$  is estimated. The value of  $E_{th}$  is higher in IT-C scenario (279 kWh<sub>th</sub>) and especially in DE-C, where it is the highest one (2,974 kWh<sub>th</sub>).

As visible from Table 7, electrical energy consumption due to ventilation is present in all the scenarios. The lowest  $E_{el}$  values are evaluated in IT-C and DE-C scenarios and they are due to the base ventilation that is performed during the cool season. The  $E_{el}$  value of ES-C scenario is considerably higher (1,542 kWh<sub>el</sub>) and it is due to both base ventilation and cooling ventilation. The  $E_{el}$  values of the scenarios that consider the warm season is relevant, being 3,117 kWh<sub>el</sub> the minimum (DE-W) and 5,047 kWh<sub>el</sub> the maximum (ES-W).

**Table 7** – Thermal ( $E_{th}$ ), electrical ( $E_{el}$ ) energy consumption and related financial costs of the considered production cycles.

Scenario	$E_{th}$ [kWh <sub>th</sub> ]	$E_{el}$ [kWh <sub>el</sub> ]	Financial costs [€]		
			Thermal energy	Electrical energy	Total
IT-C	279	614	19.50	135.19	154.69
IT-W	0	4,292	0.00	944.42	944.42
ES-C	0	1,542	0.00	339.27	339.27
ES-W	0	5,047	0.00	1,110.41	1,110.41
DE-C	2,974	613	178.44	183.89	362.33
DE-W	4	3,117	0.22	935.20	935.42

The energy consumption for climate control that can be estimated through the energy simulation model can be also useful to perform financial evaluations regarding the running costs of the pig house due to energy consumption. In Table 7, the total financial costs due to energy consumption and the shares for thermal and electrical energy are presented. The cost of energy was obtained multiplying the energy consumption by the cost of energy -including taxes- reported in Eurostat [67,68]. The cost of thermal energy was assumed equal to 0.07 € kWh<sub>th</sub><sup>-1</sup> for Italy and Spain, and 0.06 € kWh<sub>th</sub><sup>-1</sup> for Germany. The cost of electrical energy was assumed equal to 0.22 € kWh<sub>el</sub><sup>-1</sup> for Italy and Spain, and 0.30 € kWh<sub>el</sub><sup>-1</sup> for Germany. The table shows that the financial costs vary considerably between the analysed scenarios, being the range between 154.69 € (IT-C) and 1,110.41 € (ES-W). The production cycles carried out in the

warm season are the ones characterized by the highest costs that goes between 935 and 1,110 €. By contrast, the production cycles performed during the cool season are characterized by lower costs that do not exceed 362 €. An eventual improvement of the energy performance for ventilation, hence, would decrease the running costs of the pig house. In cool climate conditions, such as the ones of Germany, the running costs would benefit also from a reduction of the thermal energy consumption for supplemental heating. This is since the thermal energy share represent almost a half of the total financial cost of scenario DE-C, as visible from Table 7. To decrease the thermal energy consumption different solutions could be adopted, such as the implementation of passive heat recovery systems or the increase of the envelope thermal insulation. This last solution should be carefully evaluated since an increased thermal insulation of the envelope could lead to a potential overheating of the enclosure during the warm season and to a consequent rise of the electrical energy consumption for ventilation, as highlighted by Costantino et al. [22]. The overheating risk and the eventual increase of electrical energy consumption could be evaluated through the proposed energy simulation model.

## **7 Conclusions**

In the present work, a dynamic thermal energy simulation model for the estimation of the energy consumption and indoor climate conditions of growing-finishing pig houses was elaborated and presented. The developed model integrates the simulation of the main peculiarities of growing-finishing pig houses, such as the pig-environment interaction and the use of free-cooling systems. The reliability of the developed model was proved trough an experimental validation against real monitored data acquired through an *ad-hoc* monitoring campaign. The results were evaluated in compliance with the main protocols regarding the energy simulation of buildings that are available and well established in literature. The model resulted to be reliable in the estimation of the time profiles of the indoor climate conditions, namely air temperature and relative humidity. In addition, the model estimates with a good approximation the electrical energy consumption for ventilation.

The proposed energy simulation model contributes to fill the gap in literature that was outlined at the beginning of this work by setting a possible common methodology for the simulation of mechanically ventilated pig houses. This methodology may be extended to other types of livestock houses, such as pig farrowing rooms or laying hen houses. These simulation models, in fact, are essential for improving the energy performance of pig houses and, hence, increasing the sustainability of this agricultural sub-sector. The primary role of these models is further enhanced considering the expected population growth and the increase of animal protein

consumption. From a practical point of view, the developed model could represent a powerful decision support tool for the stakeholders involved in intensive pig production since it enhances the assessment of the energy performance of pig houses in standardized conditions. In this way, the effectiveness of new solutions, technologies and strategies aimed at increasing the energy performance of pig houses can be evaluated especially in the design stage in which fine-tuned energy-efficient solutions should be evaluated considering the specificity of the building, such as outdoor weather conditions, building configurations and farming features. This is of the foremost importance with a view on the expected climate changes. This model, in fact, may be used to evaluate the variation of energy consumption and indoor environmental conditions in different scenarios of climate change, with positive impact on the increase the resiliency of livestock houses, a strategy that is becoming essential especially in those geographical contexts which will be more affected by the climate changes. The proposed model could be adopted even in the operation stage of pig houses, providing useful data for farm management, such as running costs for energy supply and potential heat stress situations.

Future works may improve the presented energy simulation models by implementing additional calculation modules for the estimation of the energy production from renewable energy sources, such as photovoltaics and solar thermal, and for the estimation of the amount of greenhouse gas emissions due to the direct on-farm energy consumption. Furthermore, future ambitious works may couple the presented energy simulation model with a  $\text{NH}_3$ -emission model that considers further aspects of pig farming, such as feeding and other farming practices. In this way, it would be possible to make long-term estimations of  $\text{NH}_3$  emissions with the aim of evaluating the effectiveness of different emission abatement techniques, always considering the effects on the energy consumption.

## Acknowledgements

This work has been supported by financial funding of SIR (Scientific Independence of young Researchers) 2014 “EPAnHaus –Energy Performance of livestock houses” project, grant number RBSI141A3A, funded by MIUR (Italian Ministry of Education, Universities and Research).

The Authors thank the Regional Agency for the Protection of the Environment of Piemonte (ARPA Piemonte) for the outdoor weather data needed for this work and Dr. Ugo Benedetto and his staff for their willingness to take part in the project.

## References

- [1] OECD/FAO. OECD-FAO Agricultural Outlook 2019-2028. 2019. [https://doi.org/10.1787/agr\\_outlook-2019-en](https://doi.org/10.1787/agr_outlook-2019-en).
- [2] FAO. Energy-smart food for people and climate – Issue Paper. Rome: 2011.
- [3] Daramola JO, Abioja MO, Onagbesan OM. Heat Stress Impact on Livestock Production BT - Environmental Stress and Amelioration in Livestock Production. In: Sejian V, Naqvi SMK, Ezeji T, Lakritz J, Lal R, editors., Berlin, Heidelberg: Springer Berlin Heidelberg; 2012, p. 53–73. [https://doi.org/10.1007/978-3-642-29205-7\\_3](https://doi.org/10.1007/978-3-642-29205-7_3).
- [4] Moreno I, Ladero L, Cava R. Effect of the Iberian pig rearing system on blood plasma antioxidant status and oxidative stress biomarkers. *Livest Sci* 2020;235:104006. <https://doi.org/https://doi.org/10.1016/j.livsci.2020.104006>.
- [5] Gołaszewski J, de Visser C, Brodziński Z, Myhan R, Olba-Zięty E, Stolarski MJ, et al. State of the Art on Energy Efficiency in Agriculture (agrEE)- Country data on energy consumption in different agroproduction sectors in the European countries. (Project Deliverable 2.1). 2012.
- [6] Maia ASC, Culhari E de A, Fonsêca V de FC, Milan HFM, Gebremedhin KG. Photovoltaic panels as shading resources for livestock. *J Clean Prod* 2020;258:120551. <https://doi.org/https://doi.org/10.1016/j.jclepro.2020.120551>.
- [7] FAO. World Livestock 2011 - Livestock in food security. Rome: FAO; 2011.
- [8] FAO. Global agriculture towards 2050. 2009.
- [9] Pervanchon F, Bockstaller C, Girardin P. Assessment of energy use in arable farming systems by means of an agro-ecological indicator: The energy indicator. *Agric Syst* 2002;72:149–72. [https://doi.org/10.1016/S0308-521X\(01\)00073-7](https://doi.org/10.1016/S0308-521X(01)00073-7).
- [10] Jackson P, Guy JH, Sturm B, Bull S, Edwards SA. An innovative concept building design incorporating passive technology to improve resource efficiency and welfare of finishing pigs. *Biosyst Eng* 2018;174:190–203. <https://doi.org/10.1016/j.biosystemseng.2018.07.008>.
- [11] Jeong MG, Rathnayake D, Mun HS, Dilawar MA, Park KW, Lee SR, et al. Effect of a Sustainable Air Heat Pump System on Energy Efficiency, Housing Environment, and Productivity Traits in a Pig Farm. *Sustain* 2020;12. <https://doi.org/10.3390/su12229772>.
- [12] Alberti L, Antelmi M, Angelotti A, Formentin G. Geothermal heat pumps for sustainable farm climatization and field irrigation. *Agric Water Manag* 2018;195:187–299.

- <https://doi.org/10.1016/j.agwat.2017.10.009>.
- [13] Islam MM, Mun H-S, Bostami ABMR, Ahmed ST, Park K-J, Yang C-J. Evaluation of a ground source geothermal heat pump to save energy and reduce CO<sub>2</sub> and noxious gas emissions in a pig house. *Energy Build* 2016;111:446–54. <https://doi.org/10.1016/j.enbuild.2015.11.057>.
- [14] Krommweh MS, Rösmann P, Büscher W. Investigation of heating and cooling potential of a modular housing system for fattening pigs with integrated geothermal heat exchanger. *Biosyst Eng* 2014;121:118–29. <https://doi.org/10.1016/j.biosystemseng.2014.02.008>.
- [15] Axaopoulos P, Panagakis P. Energy and economic analysis of biogas heated livestock buildings. *Biomass and Bioenergy* 2003;24:239–48. [https://doi.org/10.1016/S0961-9534\(02\)00134-4](https://doi.org/10.1016/S0961-9534(02)00134-4).
- [16] Pipatmanomai S, Kaewluan S, Vitidsant T. Economic assessment of biogas-to-electricity generation system with H<sub>2</sub>S removal by activated carbon in small pig farm. *Appl Energy* 2009;86:669–74. <https://doi.org/10.1016/j.apenergy.2008.07.007>.
- [17] Axaopoulos P, Panagakis P, Axaopoulos I. Effect of wall orientation on the optimum insulation thickness of a growing-finishing piggery building. *Energy Build* 2014;84:403–11. <https://doi.org/10.1016/j.enbuild.2014.07.091>.
- [18] Costantino A, Fabrizio E. Energy modelling of livestock houses: the results from the EPAnHaus project. In: Corrado V, Fabrizio E, Gasparella A, Patuzzi F, editors. *Proc. Build. Simul. 2019 16th Conf. IBPSA, 2020*, p. 4251–8.
- [19] Tabase RK, Van linden V, Bagci O, De Paepe M, Aarnink AJA, Demeyer P. CFD simulation of airflows and ammonia emissions in a pig compartment with underfloor air distribution system: Model validation at different ventilation rates. *Comput Electron Agric* 2020;171:105297. <https://doi.org/10.1016/j.compag.2020.105297>.
- [20] Albright L. *Environmental Control for Animals and Plants*. St. Joseph: ASAE; 1990.
- [21] Jackson P, Guy J, Edwards SA, Sturm B, Bull S. Application of dynamic thermal engineering principles to improve the efficiency of resource use in UK pork production chains. *Energy Build* 2017;139:53–62. <https://doi.org/10.1016/j.enbuild.2016.12.090>.
- [22] Costantino A, Calvet S, Fabrizio E. Identification of energy-efficient solutions for broiler house envelopes through a primary energy approach. *J Clean Prod* 2021;312:127639. <https://doi.org/10.1016/j.jclepro.2021.127639>.
- [23] Pedersen S&, Sällvik K. 4th Report of Working Group on Climatization of Animal Houses – Heat and moisture production at animal and house levels. Horsens: 2002.
- [24] Costantino A, Fabrizio E, Biglia A, Cornale P, Battaglini L. Energy Use for Climate Control of Animal Houses: The State of the Art in Europe. *Energy Procedia* 2016;101:184–91. <https://doi.org/10.1016/j.egypro.2016.11.024>.
- [25] Lindley JA, Whitaker JH. *Agricultural buildings and structures*. St. Joseph: American Society of Agricultural Engineers; 1996.
- [26] Midwest Plan Service. *Structures and Environment Handbook* (11th Edition, revised 1987). Ames: Midwest Plan Service; 1983.
- [27] PIC, PIC North America. *Wean to finish manual*. 2014 editi. Hendersonville, Tennessee: PIC North

- America; 2014.
- [28] L.B. White Company. Wean-to-Finish. Heating protocol. Onalaska, Wisconsin: L.B. White Company; 2013.
- [29] Rossi P, Gastaldi A, Ferrari P. Shelters, equipment and systems for pig rearing (Ricoveri, attrezzature e impianti per l'allevamento dei suini, in Italian). Verona, Italy: Edizioni l'Informatore Agrario; 2004.
- [30] Howden SM, Crimp SJ, Stokes CJ. Climate change and Australian livestock systems: impacts, research and policy issues. *Aust J Exp Agric* 2008;48:780. <https://doi.org/10.1071/ea08033>.
- [31] Fregley MJ, Blatteis CM. *Handbook of physiology*. Oxford: Oxford University Press; 1996.
- [32] St-Pierre NR, Cobanov B, Schnitkey G. Economic Losses from Heat Stress by US Livestock Industries. *J Dairy Sci* 2003;86:E52–77. [https://doi.org/10.3168/jds.s0022-0302\(03\)74040-5](https://doi.org/10.3168/jds.s0022-0302(03)74040-5).
- [33] Esmay ME, Dixon JE. *Environmental control for agricultural buildings*. Westport: The AVI Publishing company, Inc; 1986.
- [34] Hellickson MAMA, Walker JN. *Ventilation of agricultural structures*. St. Joseph: ASAE; 1983.
- [35] Seo I hwan, Lee I bok, Moon O kyeong, Hong S woon, Hwang H seob, Bitog JP, et al. Modelling of internal environmental conditions in a full-scale commercial pig house containing animals. *Biosyst Eng* 2012;111:91–106. <https://doi.org/10.1016/j.biosystemseng.2011.10.012>.
- [36] Kwon K seok, Lee I bok, Ha T. Identification of key factors for dust generation in a nursery pig house and evaluation of dust reduction efficiency using a CFD technique. *Biosyst Eng* 2016;151:28–52. <https://doi.org/10.1016/j.biosystemseng.2016.08.020>.
- [37] Bjerg B, Rong L, Zhang G. Computational prediction of the effective temperature in the lying area of pig pens. *Comput Electron Agric* 2018;149:71–9. <https://doi.org/10.1016/j.compag.2017.09.016>.
- [38] Rong L, Aarnink AJA. Development of ammonia mass transfer coefficient models for the atmosphere above two types of the slatted floors in a pig house using computational fluid dynamics. *Biosyst Eng* 2019;183:13–25. <https://doi.org/10.1016/j.biosystemseng.2019.04.011>.
- [39] Rong L. Effect of partial pit exhaust ventilation system on ammonia removal ratio and mass transfer coefficients from different emission sources in pig houses. *Energy Built Environ* 2020;1:343–50. <https://doi.org/10.1016/j.enbenv.2020.04.006>.
- [40] Qin C, Wang X, Zhang G, Yi Q, He Y, Wang K. Effects of the slatted floor layout on flow pattern in a manure pit and ammonia emission from pit-A CFD study. *Comput Electron Agric* 2020;177:105677. <https://doi.org/10.1016/j.compag.2020.105677>.
- [41] Axaopoulos P, Panagakis P, Kyritsis S. Computer Simulation Assessment of the Thermal Microenvironment of Growing Pigs Under Summer Conditions. *Trans ASAE* 1992;35:1005–9. <https://doi.org/10.13031/2013.28694>.
- [42] Liberati P, Zappavigna P. A computer model for optimisation of the internal climate in animal housing design. *Proc. from Livest. Environ. VII Symp.*, Beijing: 2005.
- [43] Wu Z, Stoustrup J, Trangbæk K, Heiselberg P, Riisgaard Jensen M. Model Predictive Control of the Hybrid Ventilation for Livestock. *45th IEEE Conf. Decis. Control Proc.*, 2006, p. 1460–5.
- [44] Panagakis P, Axaopoulos P. Comparing fogging strategies for pig rearing using simulations to determine apparent heat-stress indices. *Biosyst Eng* 2008;99:112–8. <https://doi.org/10.1016/J.BIOSYSTEMSENG.2007.10.007>.



- [45] Xie Q, Ni JQ, Bao J, Su Z. A thermal environmental model for indoor air temperature prediction and energy consumption in pig building. *Build Environ* 2019;161:106238. <https://doi.org/10.1016/j.buildenv.2019.106238>.
- [46] Costantino A, Ballarini I, Fabrizio E. Comparison between simplified and detailed methods for the calculation of heating and cooling energy needs of livestock housing: A case study. *Build. Simul. Appl.*, vol. 2017- Febru, 2017, p. 193–200.
- [47] Coyne JM, Berry DP, Mäntysaari EA, Juga J, McHugh N. Comparison of fixed effects and mixed model growth functions in modelling and predicting live weight in pigs. *Livest Sci* 2015;177:8–14. <https://doi.org/10.1016/j.livsci.2015.03.031>.
- [48] Sabbioni A, Beretti V, Manini R, Cervi C, Superchi P. Application of different growth models to “Nero di Parma” pigs. *Ital J Anim Sci* 2009;8:537–9. <https://doi.org/10.4081/ijas.2009.s2.537>.
- [49] Wellock IJ, Emmans GC, Kyriazakis I. Describing and predicting potential growth in the pig. *Anim Sci* 2004;78:379–88. <https://doi.org/10.1017/s1357729800058781>.
- [50] Gompertz B. On the nature of the function expressive of the law of human mortality, and on a new mode of determining the value of life contingencies. *Philos Trans R Soc London* 1825.
- [51] European Committee for Standardisation, EN ISO. EN ISO 13790: Energy performance of buildings– Calculation of energy use for space heating and cooling. 2008.
- [52] Marchio D, Millet JR, Morisot O. Simple modelling for energy consumption estimation in air conditioned buildings. *Proc. Clima 2000*, Brussel, Belgium: 1997.
- [53] Roujol S, Fleury E, Marchio D, Millet JR, Stabat P, Paris M De, et al. Testing the energy simulation building model of consoclim using bestest method and experimental data. *Conférence IBPSA World*, Eindhoven, 2003, p. 1131–8.
- [54] Costantino A, Fabrizio E, Ghiggini A, Bariani M. Climate control in broiler houses: A thermal model for the calculation of the energy use and indoor environmental conditions. *Energy Build* 2018;169. <https://doi.org/10.1016/j.enbuild.2018.03.056>.
- [55] Costantino A, Comba L, Sicardi G, Bariani M, Fabrizio E. Energy performance and climate control in mechanically ventilated greenhouses: A dynamic modelling-based assessment and investigation. *Appl Energy* 2021;288:116583. <https://doi.org/https://doi.org/10.1016/j.apenergy.2021.116583>.
- [56] Ballarini I, Costantino A, Fabrizio E, Corrado V. The dynamic model of EN ISO 52016-1 for the energy assessment of buildings compared to simplified and detailed simulation methods. In: Corrado V, Fabrizio E, Gasparella A, Patuzzi F, editors. *Proc. Build. Simul. 2019 16th Conf. IBPSA*, 2020, p. 3847–54.
- [57] Costantino A, Fabrizio E, Villagrà A, Estellés F, Calvet S. The reduction of gas concentrations in broiler houses through ventilation: Assessment of the thermal and electrical energy consumption. *Biosyst Eng* 2020;199:135–48. <https://doi.org/10.1016/j.biosystemseng.2020.01.002>.
- [58] Cattarin G, Pagliano L, Causone F, Kindinis A, Goia F, Carlucci S, et al. Empirical validation and local sensitivity analysis of a lumped-parameter thermal model of an outdoor test cell. *Build Environ* 2018;130:151–61. <https://doi.org/https://doi.org/10.1016/j.buildenv.2017.12.029>.
- [59] Xin H, Harmon JD. *Livestock Industry Facilities and Environment: Heat Stress Indices for Livestock*. *Agric Environmental Ext Publ* 1998;163. <https://doi.org/10.1007/BF02978744>.

- [60] Mikovits C, Zollitsch W, Hörtenhuber SJ, Baumgartner J, Niebuhr K, Piringer M, et al. Impacts of global warming on confined livestock systems for growing-fattening pigs: simulation of heat stress for 1981 to 2017 in Central Europe. *Int J Biometeorol* 2019;63:221–30. <https://doi.org/10.1007/s00484-018-01655-0>.
- [61] Teshome EJ, F. Haghghat F. Zonal Models for Indoor Air Flow - A Critical Review. *Int J Vent* 2004;3:119–29. <https://doi.org/10.1080/14733315.2004.11683908>.
- [62] ANSI/ASHRAE. ASHRAE Guideline 14-2002 Measurement of Energy and Demand Savings. Ashrae 2002.
- [63] IPMVP New Construction Subcommittee. International Performance Measurement & Verification Protocol: Concepts and Option for Determining Energy Savings in New Construction, Volume III. Washington, DC, USA: 2003.
- [64] Federal Energy Management Program. Federal Energy Management Program, M&V Guidelines: Measurement and Verification for Federal Energy Projects Version 3.0. 2008.
- [65] European Commission. Pig Market Situation. Pigmear C Comm 22 April 2021 2021. [https://ec.europa.eu/info/sites/default/files/food-farming-fisheries/farming/documents/pig-market-situation\\_en.pdf](https://ec.europa.eu/info/sites/default/files/food-farming-fisheries/farming/documents/pig-market-situation_en.pdf) (accessed May 17, 2021).
- [66] Fernandez MD, Losada E, Ortega JA, Arango T, Ginzo-Villamayor MJ, Besteiro R, et al. Energy, Production and Environmental Characteristics of a Conventional Weaned Piglet Farm in North West Spain. *Agron* 2020;10. <https://doi.org/10.3390/agronomy10060902>.
- [67] Eurostat. Natural gas price statistics 2020. [https://ec.europa.eu/eurostat/statistics-explained/index.php?title=Natural\\_gas\\_price\\_statistics](https://ec.europa.eu/eurostat/statistics-explained/index.php?title=Natural_gas_price_statistics) (accessed February 16, 2021).
- [68] Eurostat. Electricity price statistics 2020. [https://ec.europa.eu/eurostat/statistics-explained/index.php/Electricity\\_price\\_statistics](https://ec.europa.eu/eurostat/statistics-explained/index.php/Electricity_price_statistics) (accessed February 17, 2021).